8-2016

3D Seismic Interpretation of Paleokarst Sinkholes, Boone Limestone, Lower Mississippian: Subsurface Eastern Arkoma Basin, Conway County, Arkansas

Daniel James Moser
University of Arkansas, Fayetteville

3D Seismic Interpretation of Paleokarst Sinkholes, Boone Limestone, Lower Mississippian: Subsurface Eastern Arkoma Basin, Conway County, Arkansas

A thesis submitted in partial fulfillment
of the requirements for the degree of
Master of Science in Geology

by

Daniel J. Moser
University of Texas at San Antonio
Bachelor of Science in Geology, 2013

August 2016
University of Arkansas

This thesis is approved for recommendation to the Graduate Council

_____
Dr. Christopher Liner
Thesis Director

_____
Dr. Walter L. Manger
Committee Member

_____
Dr. Doy Zachry
Committee Member

_____
Steve Milligan
Committee Member

Abstract

Unconventional natural gas discoveries in the Fayetteville Shale of the eastern Arkoma Basin have led to improved understanding of subsurface geology in central Arkansas. This study interprets 3D seismic data for evidence of paleokarst within the Mississippian formations in a portion of the subsurface of Conway County, Arkansas. Quantitative data interpretation suggests that sinkholes developed during the Mississippian portion of the eastern Arkoma Basin record.

In a nine square mile area, 3D seismic mapping of Mississippian formations show 14 closed depressions interpreted as karst sinkholes. Time and depth structure maps were created and utilized to estimate the timing of dissolution and infill of the sinkholes. Measuring the size and morphology for each sinkhole, histograms were made to summarize sinkhole characteristics. Sinkhole areas in the Boone Limestone correspond to areas of low acoustic impedance, likely indicating enhanced porosity due to fractures and dissolution.

Scale of the observed sinkholes suggests that they are consistent with modern solution sinkholes. Sinkholes in the study area occupied 10.7% of the entire Boone Limestone surface. Structure maps suggest that dissolution and collapse of the Boone continued throughout the marine transgression and deposition of both the Moorefield Shale and Hindsville Limestone in the Meramecian and early Chesterian. Final filling was accomplished during the deposition of the Fayetteville Shale in the late Chesterian. Regionally, sinkholes developed in early Ordovician carbonates have been filled with late Pennsylvanian sediments.

Acknowledgements

"The difference between a successful person and others is not the lack of strength, not a lack of knowledge, but rather a lack of will." ~Vince Lombardi

The research was only possible through the generous donation of the Desoto 3D seismic and well data by SWN, facilitated by Mr. Damien Friend. Additional well and seismic tie information was kindly supplied Mr. Joel Greer of SWN.

I would like to give a special thanks to my thesis advisor and committee chairman, Dr. Christopher Liner, for setting me up with this incredible research opportunity and guiding me along the way. This thesis would have been impossible without your assistance. Thank you for all of your patience, motivation, and immense geophysical knowledge these past two years. I would like to thank the rest of my thesis committee: Dr. Walter Manger, Dr. Doy Zachry, and Steve Milligan. It was a pleasure working with some of the most respected geologists at the University of Arkansas. Your knowledge and passion for geology is truly inspiring, and motivates me to become a better geologist. You have all taught me so much and I am extremely grateful.

Thanks to the University of Arkansas MarkUp team for your help and advice on the completion of this thesis.

Special thanks to Laura Bennett for all of your encouragement, advice, and help with my thesis edits this past year.

Lastly, but most, I would like to thank my family. I am truly blessed to have such a loving and caring family to rely on for their support, encouragement, and endless amount of prayers.

Dedication

This is dedicated to my grandparents, Jim and Virginia Moser, who have been a big part of my life, and have always made the effort to attend my activities. To my grandmother, Myrtle Scarlato, who loves me unconditionally, and to the memory of my grandfather, William C. Scarlato. This is also to my parents, Jim and Rose Moser, for their love and endless support throughout my life. I wouldn't be where I am today without all of you.

Table of Contents

List of Figures

List of Tables

INTRODUCTION

A. Purpose of Study

Natural gas was discovered in the Arkoma Basin in 1887 and has played a significant role in the interest of research. Following the discovery, the first commercial development began in March, 1902, in Sebastian County, Arkansas and production increased markedly afterward (Fayetteville, 2015). The Atoka sandstone was the primary formation for natural gas production until horizontal drilling and hydraulic fracturing was developed to produce from tighter formations. The Fayetteville Shale, previously known as the source rock of the Atoka, became a productive reservoir after 2004, when Southwestern Energy drilled a horizontal well in the Fayetteville Formation in Conway County, Arkansas. The discovery well, Thomas 1-9, is located near Jerusalem, Arkansas (Taylor, 2016). By 2013, Arkansas was the eighth leading state for natural gas production and was producing approximately one trillion cubic feet per year from the Fayetteville Formation (Fayetteville, 2015). The rapid growth of production since 2004 has resulted in the drilling of thousands of wells in the eastern Arkoma Basin. Surface locations are marked in the eastern Arkoma Basin, where wells have been drilled, targeting natural gas in the Fayetteville Shale (Figure 1). Subsurface interpretation brought about by the information provided by these wells has contributed to a better understanding of the geology and structure in the surrounding area. The intention of the current work is to further subsurface investigations using 3D seismic.

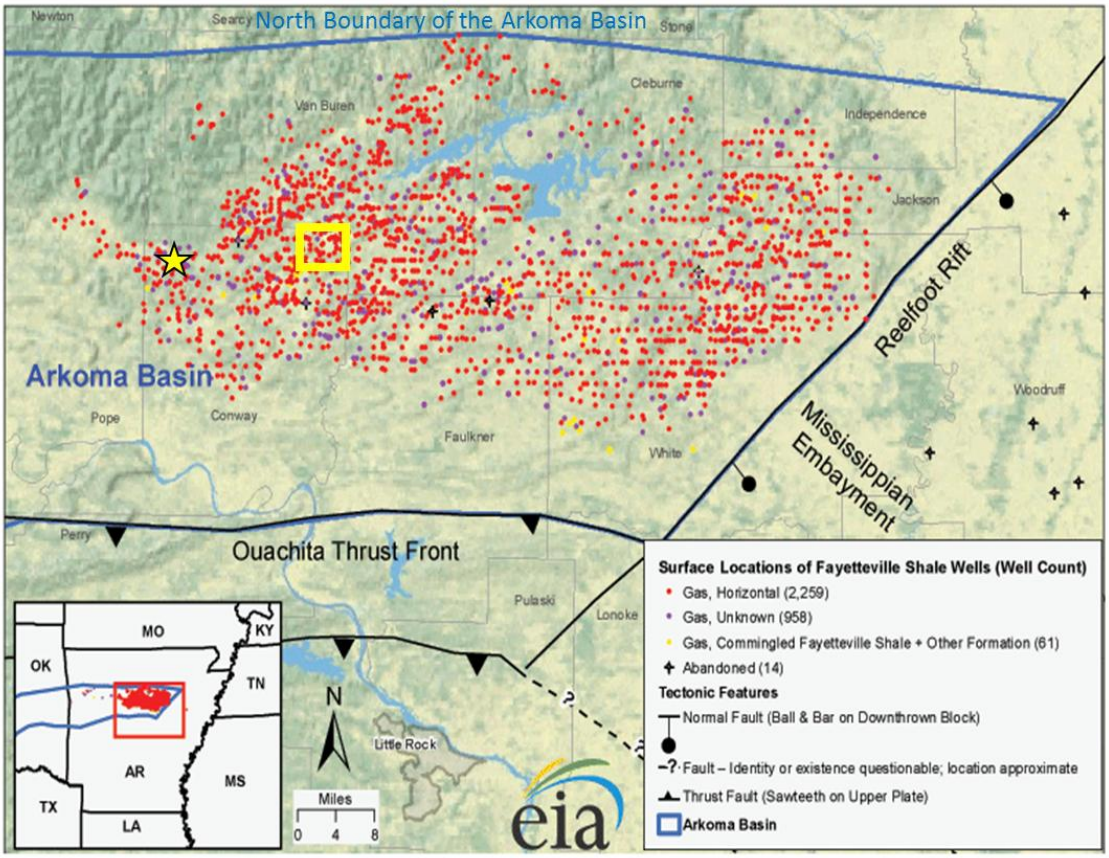

Figure 1. Eastern Arkoma Basin section with the location of Fayetteville Shale wells. Yellow box denotes the study area. Star indicates location of discovery well. Modified from (EIA, 2016).

For this study, Southwestern Energy provided the Desoto 3D seismic survey in the northeast corner of Conway County, Arkansas (Figure 2). Conway County is located in central Arkansas, which is a part of the eastern Arkoma Basin. Below the Mississippian-Pennsylvanian boundary, abundant surface depressions are noticeable in the seismic data, all terminating at the Mississippian-Pennsylvanian boundary (Figure 3). There are 14 of these subsurface depressions in the survey area that are interpreted as paleokarst sinkholes. In figure 3, the deepest sinkhole in the area is shown with estimated maximum depth of 60 ft. This study intends to provide a comprehensive 3D seismic interpretation of the study area in Mississippian strata where the sinkhole structures occur. Formations studied include the Boone Limestone, Moorefield Shale, Hindsville Limestone, Lower-Middle Fayetteville Shale, and the Upper Fayetteville Shale. By interpreting structural features and horizons in 3D seismic, this study analyzes the relationship between periods of deposition and formation of the sinkholes. Additionally, an analysis is given to determine the type of sinkholes that had formed in the early Mississippian. This will lead to a better understanding of the depositional history and environment of the eastern Arkoma Basin.

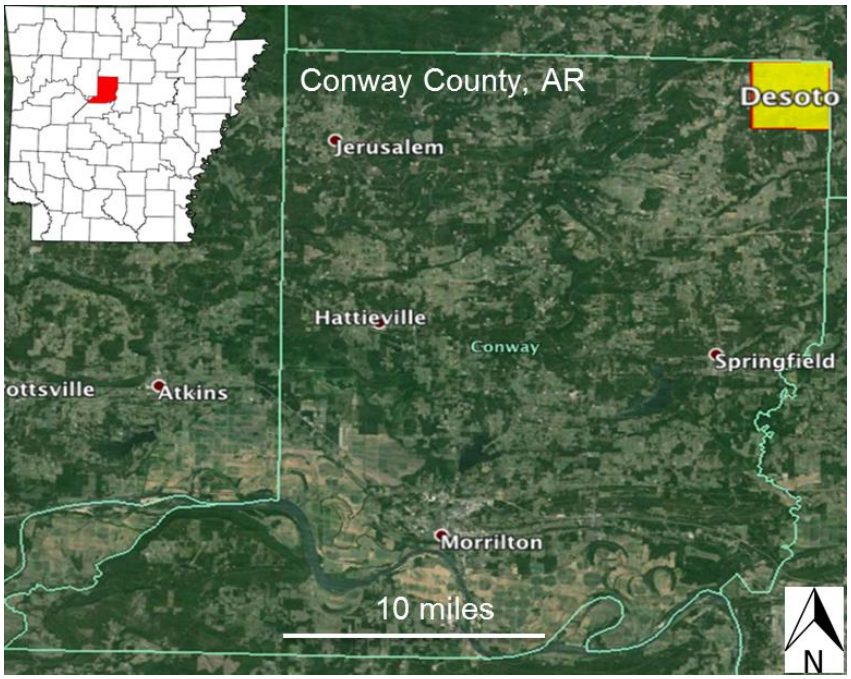

Figure 2. Google Earth map of Conway County, Arkansas. The yellow box in the northeast corner denotes location of the 3D seismic survey.

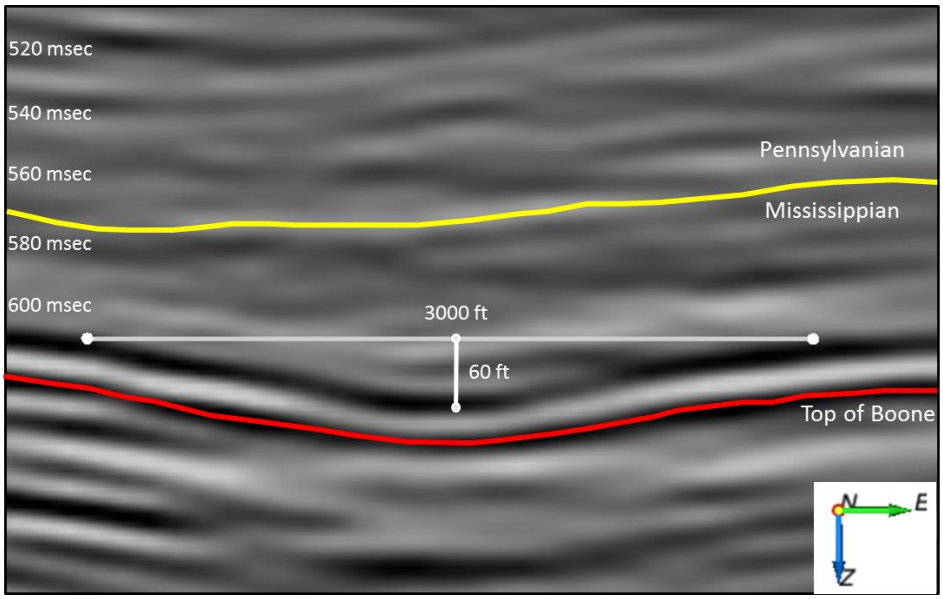

Figure 3. Higher magnification view of crossline 1619 demonstrating a depression feature, interpreted as a paleokarst sinkhole in the Boone Limestone.

B. Previous Investigations

Analysis of deeply buried karst features in the Arkoma Basin of Arkansas has not been described in the literature. However, karst features have been recognized on the surface and in outcrops in the Ozark region. In northern Arkansas, most of the sinkholes are developed from dissolution in the Boone Limestone. Sinkholes that occur in the Boone are typically solution subsidence or collapse sinkholes overlain by a thin layer of Batesville Sandstone (Chandler, 2013). Sinkholes in the Boone Limestone have been recognized on the surface in northern Arkansas, such as in Marion, County (Chandler, 2013; Figure 4a). One of the larger sinkholes found was 30-40 ft deep, and 40-50 ft in diameter, described as a conical solution sinkhole (A. Chandler, personal communication). Figure 4b shows another sinkhole in the Ozark region exposed along a road cut off of Interstate 44 in Rolla, Missouri. This outcrop shows Pennsylvanian sediment filling in sinkholes that were preserved in the lower Ordovician. The Mississippian section had been removed by later erosion farther up on the Ozark Dome. Before erosion, it is very likely the Boone limestone would have also contained sinkhole development.

Paleokarst features have also been studied in the Oklahoma portion of the Arkoma Basin. Mike Kumbalek (2015) interpreted and mapped 651 sinkholes within the Viola Limestone in a 3D seismic survey in Coal and Hughes County, Oklahoma. The Viola Limestone is a Late Ordovician rock. Sinkholes in the Viola are associated with the Viola/Sylvan unconformity within the Late Ordovician. Based on his analysis, sinkholes in the Viola Limestone are generally compound and cockpit sinkholes. Sinkholes in the Viola Limestone are older than the sinkholes analyzed in this study.

a)

b)

Figure 4. (a) Sinkhole in the Boone limestone in Marion County, AR. Modified from (Chandler, 2013). (b) Outcrop of a sinkhole fill in Rolla, Missouri. Modified from (Manger, 2016).

GEOLOGICAL HISTORY

A. Geologic Setting

The Arkoma Basin is one of several foreland basins that formed along the Ouachita Orogenic Belt during the Mississippian and Pennsylvanian periods (Suneson, 2012). It covers approximately 33,800 square miles and extends from southeastern Oklahoma to central Arkansas (Perry, 1994). The Arkoma Basin is bounded to the north by the Ozark Uplift, to the south by the Ouachita Mountains, to the northwest by the Anadarko Basin, to the southwest by the Arbuckle Uplift, and to the southeast by the Mississippian Embayment (Figure 5). The red box in figure 5 denotes the general location of the study area, which is in the eastern Arkoma section.

At the surface, the basin is comprised of broad synclines that are separated by narrow anticlines (Viele, 1973). In the subsurface, three structural styles of faulting are evident from the Proterozoic basement to Pennsylvanian strata. These include steeply dipping basement normal faults, shallow listric normal faults, and thrust faults. The structural framework was controlled by multiple tectonic events and subsequent deposition. This foreland tectonic basin was created by rifting and subsequent collision of the North American and Gondwanan plates, followed by the uplift of the Ouachita thrust belt. All of the Mississippian sediments were deposited on a broad, stable shelf throughout its depositional history, prior to continental convergence (Sutherland, 1988). These sediments consist of shallow marine carbonates, quartz sandstones, and shales.

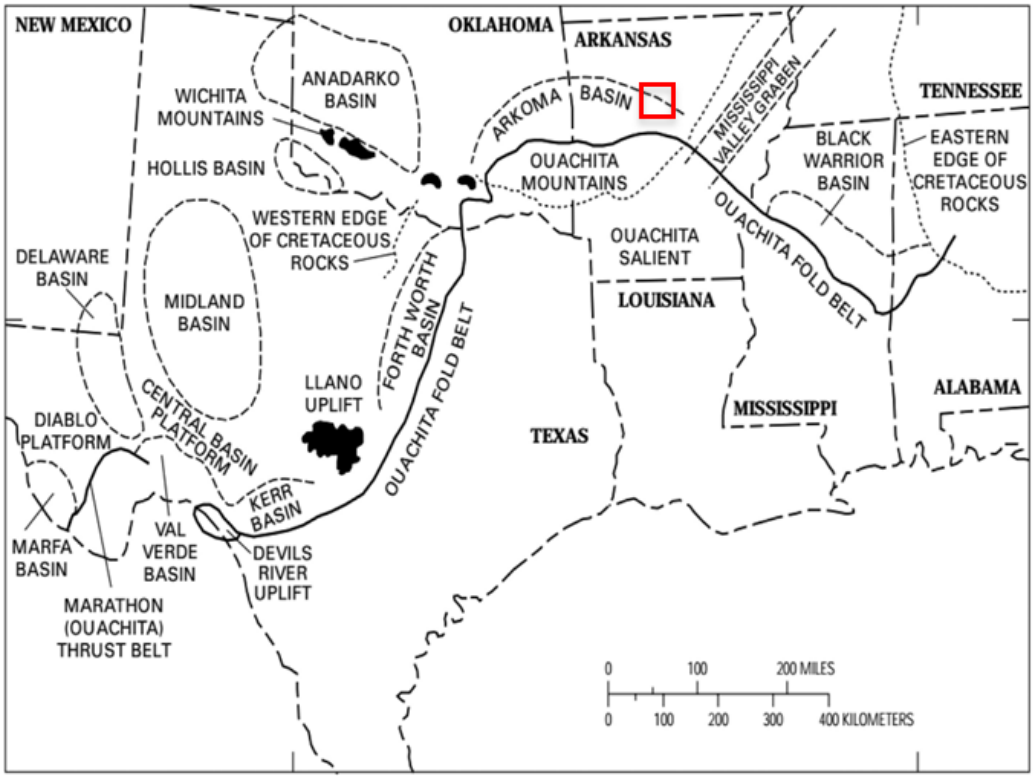

Figure 5. Regional map displaying the foreland basins in the southern midcontinent. The red box denotes the general location of the study area. Modified from (Suneson, 2012).

B. Lithostratigraphy

Generalized stratigraphic succession of the eastern Arkoma Basin is illustrated in Figure 6 that highlights the Mississippian strata in this study (Horton, 2012). Figure 6 also points out the major tectonic events the led to the formation of the Arkoma Basin. Formations from the Upper Cambrian to the Lower Pennsylvanian were deposited along the shelf of the passive margin prior to the Ouachita Orogeny. Lower Pennsylvanian to Middle Pennsylvanian strata were deposited in the basin after vertical loading and uplift of the Ouachita Mountains. The rocks are thickest along the southern margin of the basin, with a maximum thickness of approximately 5,000 ft. Stratigraphic sections generally thin upward towards the north by thinning, depositional onlap, and erosion (Houseknecht *et al*., 2014). The basin is mostly comprised of shallow marine sediments that were deposited along the shelf, containing sequences of carbonates, shales, and quartz sandstones.

Formations of interest in this research are the Mississippian units consisting of the Boone Limestone, Moorefield Shale, Hindsville Limestone, Lower-Middle Fayetteville Shale, and Upper Fayetteville Shale. The Boone is a fine to coarse grained, gray fossiliferous limestone with interbedded chert. This formation is known to contain "dissolution structures, such as sinkholes, caves, and enlarged fissures" (Ozark, 2016). It rests unconformably above the Chattanooga Shale and unconformably below the Moorefield Shale in the eastern Arkoma Basin. The Boone is approximately 300 feet thick is the survey area. The Moorefield is approximately 70 ft thick and contains a lower member of interbedded black shale with siliceous limestone and an upper member of dark calcareous and phosphatic shale (Manger, 2015). The Boone-Moorefield contact is

typically distinct across the Arkoma Basin. In some areas the base of the Moorefield can be calcareous, creating a gradational contact with the Boone Limestone (Manger, 2015). South and east of the northern Arkoma Basin, this contact is apparent in the subsurface as the Boone thins and becomes shaly (Shelby, 1986). This gradational contact is observed at the top of the Boone in the gamma ray log. The Hindsville Limestone is a member of the Batesville Sandstone. The Hindsville is a crystalline, fossiliferous limestone composed of ooliths, crinozoans, and brachiopodal detritus cemented by calcite spar (Manger, 2015). It is very thin in the survey area (approximately 15 feet). The Wedington Sandstone in western Arkansas separates the Upper and Lower Fayetteville, and pinches out towards the east before Conway County. Fayetteville Shale in the area is separated into a lower, middle, and upper sections. The Lower Fayetteville is a fissile black shale. Combined in the survey area, the Lower to Middle Fayetteville interval is 170 feet thick and organically rich. This section can be distinguished from the Upper Fayetteville Shale by its very high radioactivity and high resistivity log signatures (Ratchford and Bridges, 2006). The Upper Fayetteville shale is approximately 120 feet thick in the survey area. It is a concretionary black shale that contains benthonic fauna dominated by bivalve mollusks and cephalopods (Manger, 2015). Above the Upper Fayetteville in the survey area is the Morrowan Shale. The light gray, oolitic Pitkin Limestone typically overlies the Upper Fayetteville, but is absent in the survey area.

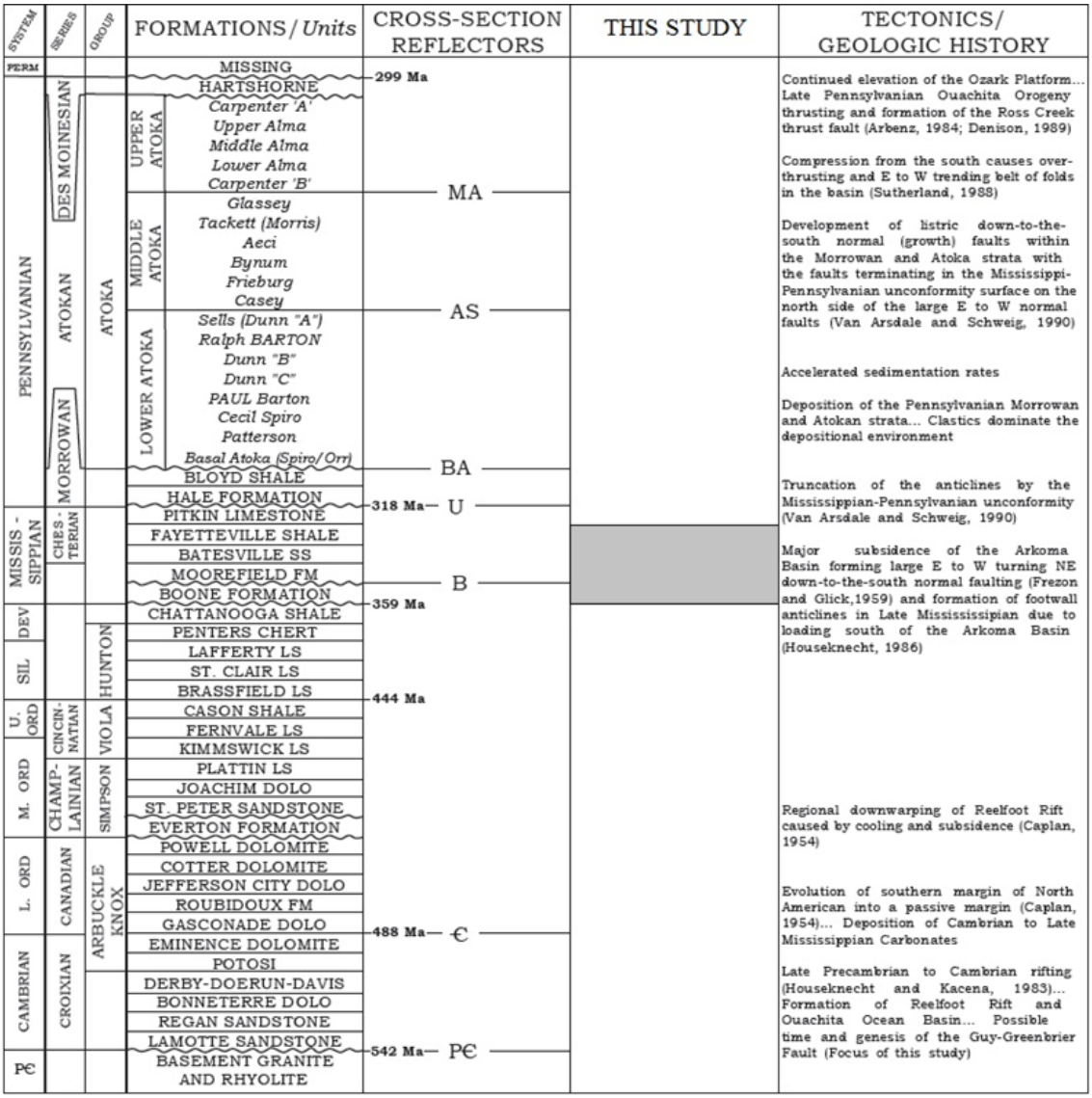

Figure 6. Stratigraphic column for the Eastern Arkoma Basin displaying the regional tectonic events and Mississippian formations in this study. Modified from (Horton, 2012).

C. Structural Framework

The eastern Arkoma Basin has a surface structure that is dominated by northeast-trending normal faults, upright northeast trending folds, and the Ross Creek thrust fault (Van Arsdale and Schweig, 1990). The surface also contains broad synclines separated by narrow anticlines as described by Viele (1973). Beginning with continental rifting during the Precambrian, this structural design was influenced by subsequent tectonic events and deposition until the uplift of the Ouachita Mountains. An analysis of the subsurface structure of the eastern Arkoma Basin was interpreted by Van Arsdale and Schweig (1990) using 425 km of seismic reflection data. Their survey is located in four counties southeast of my study area in Van Buren, Faulkner, Cleburne, and White County (Figure 7). Figure 8 shows the two-way structure map of the Boone Formation in relation to the study area denoted by the yellow box (Van Arsdale and Schweig, 1990). According to the time structure map, the Boone Formation is sloping towards the southwest with multiple styles of faults. Faults closest to the study area generally strike east and northeast, and dip south to southeast. This attitude suggests that a similar structural pattern may be exhibited in the study area.

The overall seismic interpretation of Van Arsdale and Schweig (1990) focuses on three structural regimes in the eastern Arkoma Basin, as illustrated by the cross section in Figure 9 (Van Arsdale and Schweig, 1990). Symbols in the cross section are referenced in the stratigraphic column in Figure 6. The structural systems include (1) deep, steeply dipping normal faults; (2) shallow listric normal faults; and (3) thrust faults associated with folds (Van Arsdale and Schweig, 1990). Descriptions of the structural deformation are:

(1) The deep, steeply dipping normal faults extend upward from the Proterozoic basement through the Pitkin Limestone and terminate at the Morrowan Series (Figure 9). Termination of the faults are due to the eroded surface at the base of the Pennsylvanian. Minor horsts and grabens are visible on the hanging-wall blocks, with footwall blocks tilted down to the north and deformed into anticlines. Following the deposition of Cambrian through Mississippian strata, these normal faults and anticlines had formed from the Ouachita thrust loading south of the Arkoma Basin (Houseknecht, 1986). Truncations of the anticlines are evident at the Mississippian-Pennsylvanian unconformity.

(2) Shallow listric normal faults displace the Pennsylvanian strata upward from the Morrowan through the Atokan formations, and are overlain by narrow anticlines (Figure 9). These shallow-dipping normal faults merge into the truncated surface of the Morrowan Series and do not penetrate the deeper normal faults. They are related to deformation of the Arkoma Basin. With the progression of the overriding plate during the Early Atokan, the continent experienced flexural bending and subsidence, which resulted in the listric normal faults throughout the area.

(3) Following the deposition of the Morrowan through the Atokan formations came the Ouachita Orogeny thrusting event that led to the formation of the Ross Creek Thrust fault (Van Arsdale and Schweig, 1990).

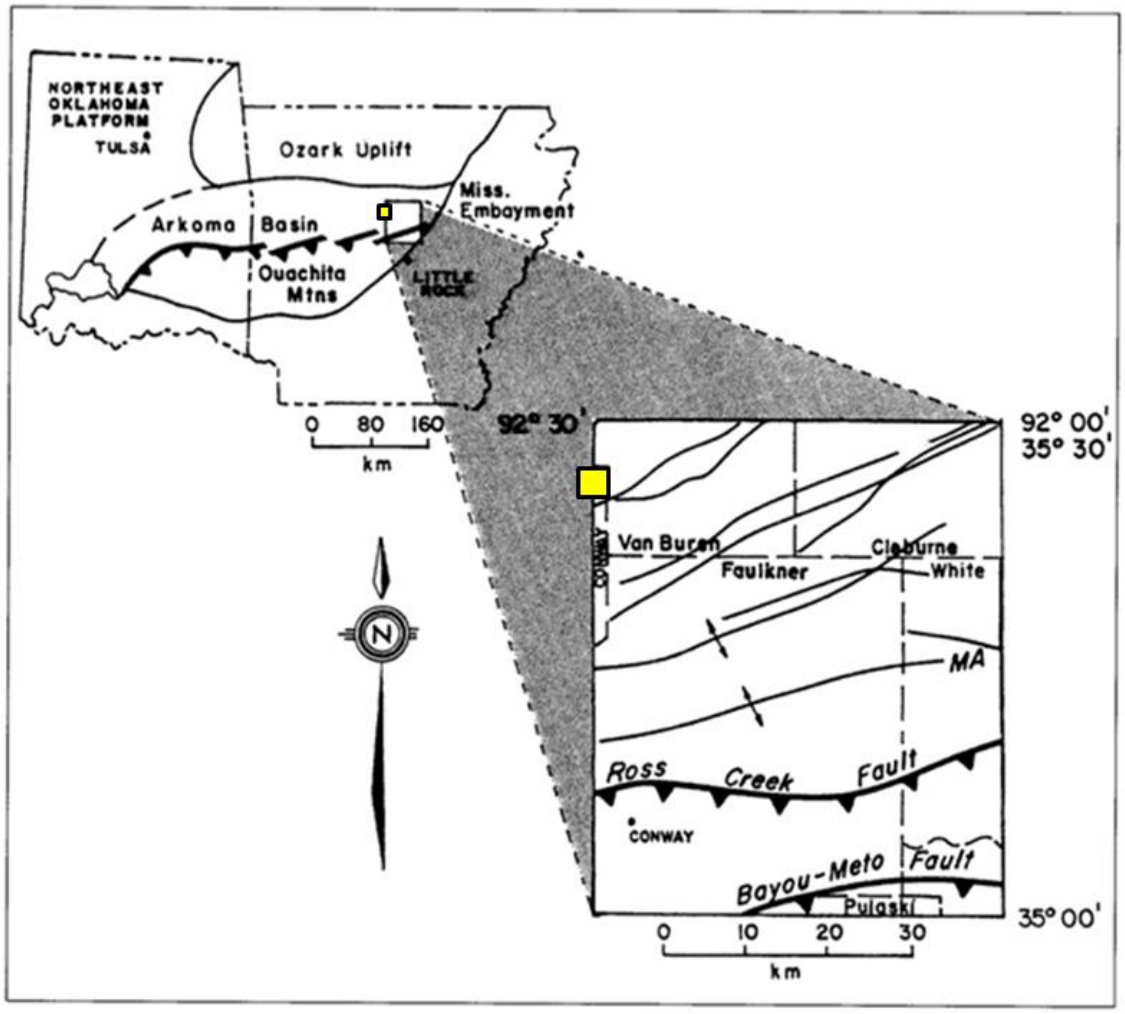

Figure 7. Survey location for Van Arsdale and Schweig (1990) in the Eastern Arkoma Basin. Yellow box denotes the study area. Thin lines represent faults. MA = Morrilton Anticline.

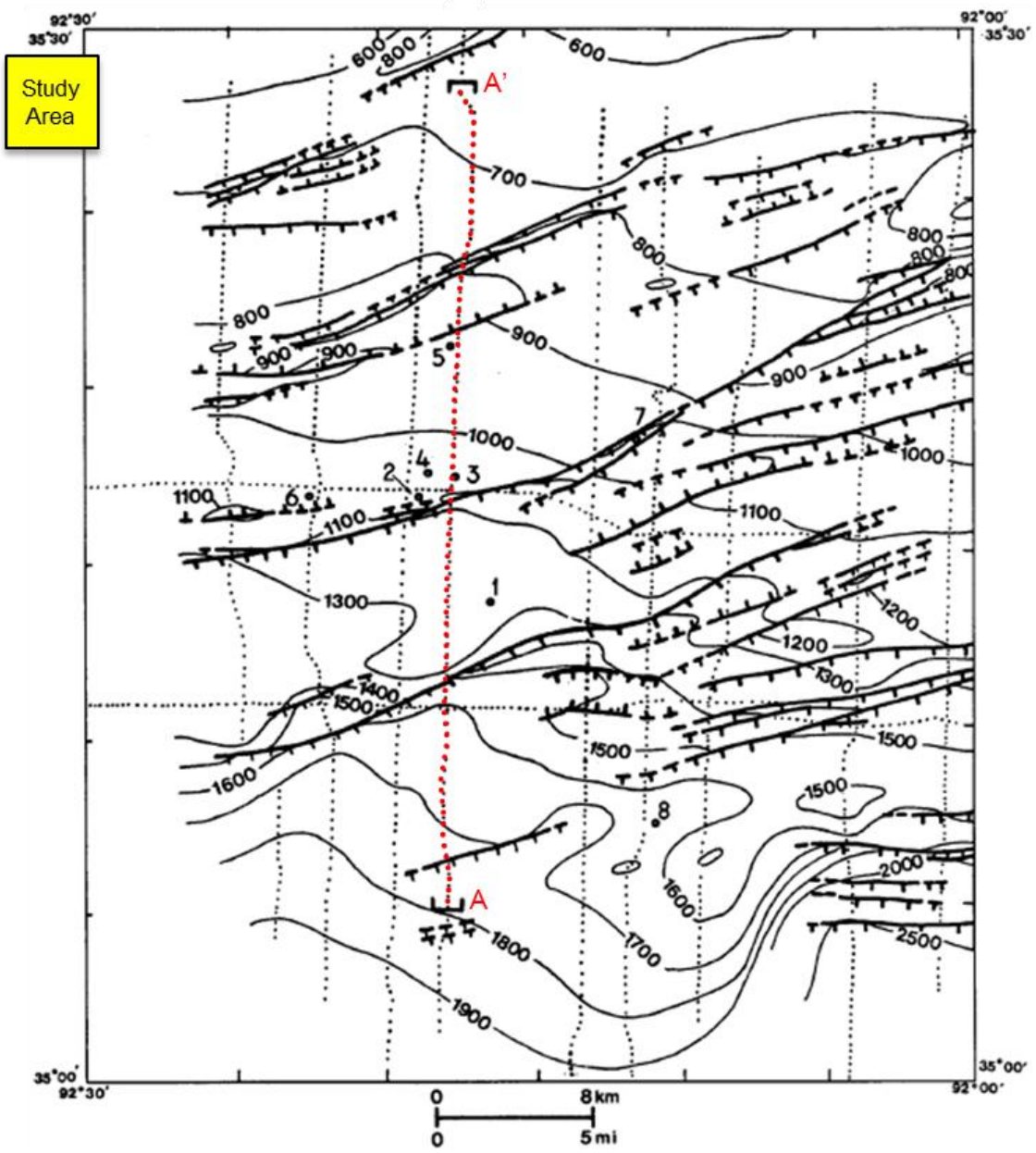

Figure 8. "Time structure map of the Boone Formation using two-way time. Bold lines are normal faults, barbs on downthrown side. Dotted lines are the location of the seismic reflection lines. Line AA' represents the cross section shown in Figure 9. The numbered points are the following gas exploration wells: 1 = Lone Star 1 E.W. Moore Estate, 2 = Arco Exploration 1 Wayne L. Edgmon, 3 = Santa Fe Energy 1-29 Mary Lou, 4 = Stephens Production 1 S.A. Hovis, 5 = Sepco 1-8B Brown, 6 = Santa Fe Energy 1-4 Sowash, 7 = Diamond Shamrock 1 Rushing, 8 = Shell Oil 1-28 Atkinson." Modified from (Van Arsdale and Schweig, 1990).

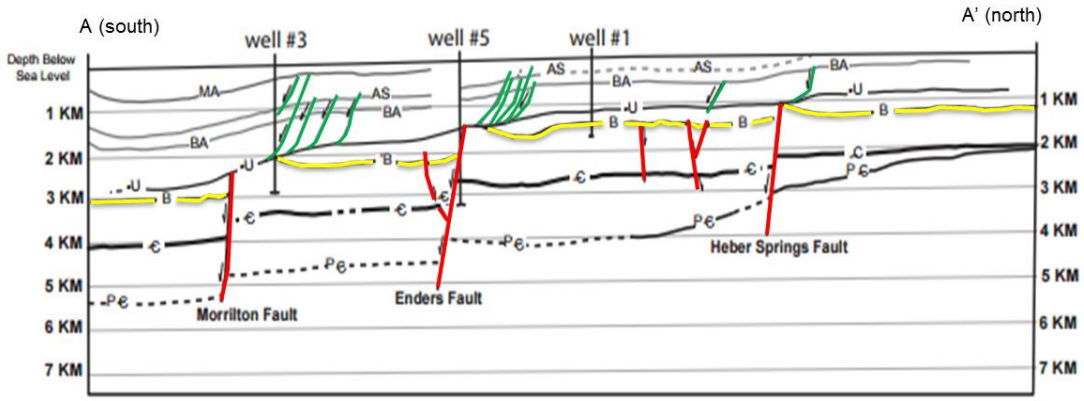

Figure 9. Cross section line of A-A' and geological interpretation. Boone Formation is highlighted in yellow. Red lines denote deep, steeply dipping normal faults. Green lines denote shallow listric normal faults. Reflectors are identified in the stratigraphic column shown in figure 6. Wells #3, #5 and #1 are waste disposal wells. Modified from (Van Arsdale and Schweig, 1990; Horton, 2012).

D. Tectonic Evolution

A five-stage tectonic model created by Houseknecht (1986) illustrates the tectonic evolution and sedimentation that developed the Arkoma Basin, as well as the transition of a passive continental margin into a foreland basin shown in Figure 10. During the Precambrian through middle Cambrian, a major rifting event took place between the southern margin of North America and Llanoria, resulting in the opening of a new proto–Atlantic ocean basin called the Iapetus Ocean (Figure 10a). Various small rift basins were developed along this margin, including the Reelfoot Rift Basin and the Ouachita Ocean Basin (Houseknecht and Kacena, 1983). The Reelfoot Basin underwent continuous rifting during the Early and Middle Cambrian, but became inactive shortly after the Anadarko Basin developed as an aulocogen. The strata within both the Arkoma and the Anadarko Basins are the best known remnants from the rifting tectonic event.

The southern margin of North America evolved into a south-sloping, passive Atlantic-type margin by the Early Ordovician. This created the conditions for widespread deposition of shallow marine carbonates along the shelf (Figure 10b). A prism of sediment was formed from deposition of sediments and created a rise in the slope geometry. Sequences of shallow-water carbonates, shales, and quartzose sandstones were deposited along this shelf until the Atokan (Houseknecht, 1986). These are known as the Ouachita facies because they were later thrusted upwards during the Ouachita Orogeny and are now seen in outcrops in the Ouachitas. As the mid-ocean ridge drifted southward away from the continental margin, subsidence occurred in the area from thermal cooling (Houseknecht and Kacena, 1983).

In the Mississippian, the rifted plates began to converge, closing the Iapetus Ocean and completing a full Wilson Cycle (Figure 10c). As the North American plate submerged beneath the South American plate, the Ouachita orogenic belt began to form as an accretionary prism. The continent was subjected to major subsidence throughout the area, and initiated the formation of northeast, down to the south, steeply dipping normal faults. Loading from the overriding plate created the formation of footwall anticlines.

By the Early Atokan, progression of the overriding South American plate increased the vertical loading on the southern margin of North America, resulting in flexural bending and increased subsidence. This led to widespread normal faulting throughout the region. The majority of faults strike north-south, parallel to the Ouachita trend (Houseknecht, 1986). As seen in Figure 10d, the "shelf-slope-rise geometry" that had previously formed was disrupted by normal faults and transitioned into a step-like foundation (Houseknecht, 1986). As sedimentation increased, these growth faults were filled by deposition of Early through Middle Atokan sediments.

Uplift along the Ouachita thrust belt by the late Atokan time period completed the formation of the Arkoma Basin (Figure 10e). The deep basin had been filled by sedimentation, and major structural deformation of the Arkoma followed (Houseknecht and Kacena, 1983).

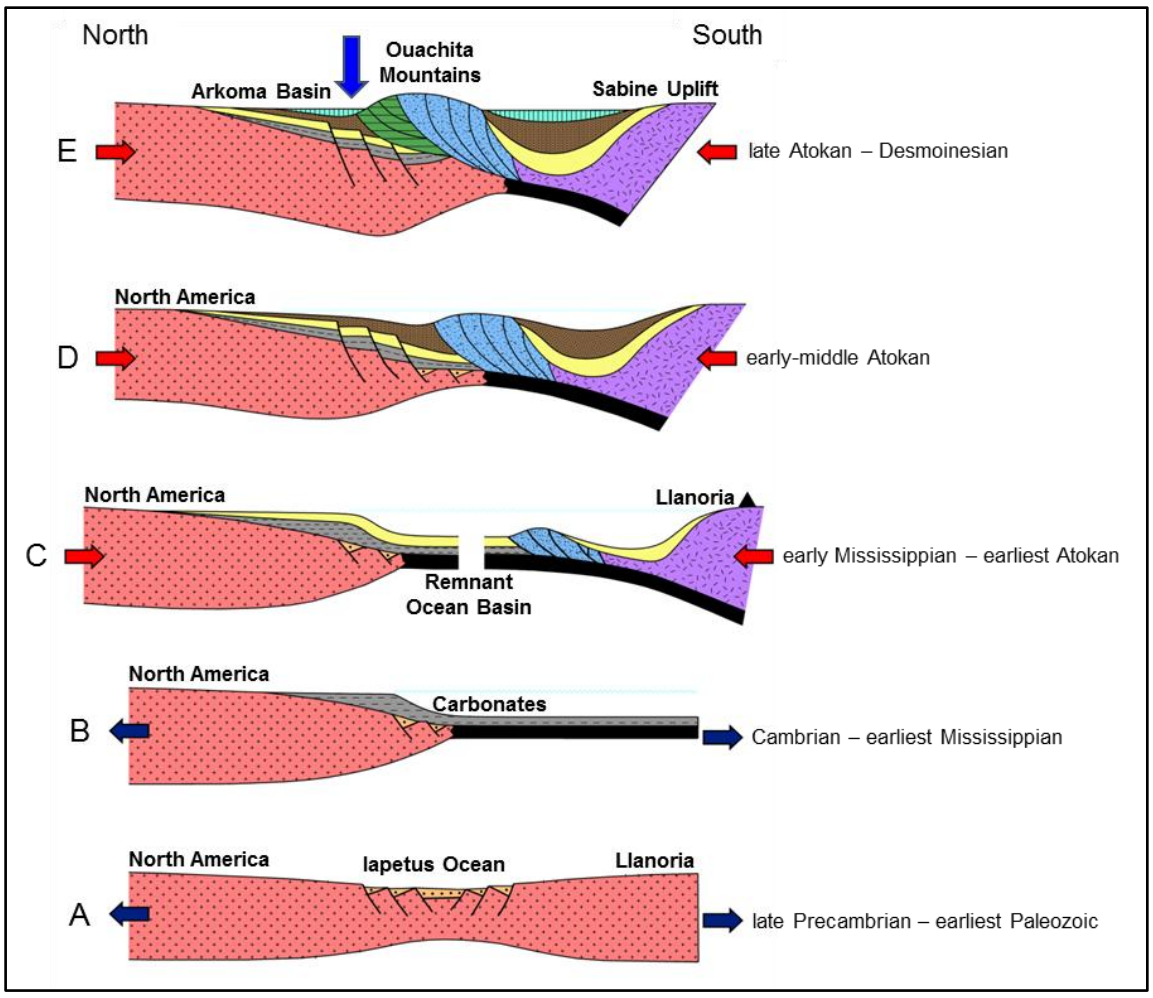

Figure 10. Cross section illustrating the five distinct stages of tectonic evolution and depositional history of the Arkoma Basin and uplift of the Ouachita Mountains. Blue arrow denotes the general location of the study area. Modified from (Houseknecht, 1986; Rogers, 2012).

E. Depositional Setting

Before Atokan time, sediments were deposited on a stable shelf along a passive continental margin. Arkansas experienced a warm shallow marine, depositional environment from Early to Late Mississippian (Figure 11). The Arkoma Basin was located on the south edge of the North American plate, approximately 10°-12° S latitude (Figure 12). Shallow water carbonates, chert, and thin deep-water black shales accumulated on the shelf in the Cambrian to Early Mississippian (Sutherland, 1988), but conditions had changed by the Middle Mississippian. Deposition of thick turbdites fed longitudinally from east to west across the basin are known as the Stanley Group in the Ouachita trough (Sutherland, 1988). Sea level gradually transgressed from the Middle to Late Mississippian. The end of the Mississippian is marked by an unconformity, which represents the boundary between the Mississippian and Pennsylvanian Periods. The Pennsylvanian was marked by a major sea withdrawal throughout the southern mid-continent region as a result of the broad upwarping of the transcontinental arch (Rascoe and Adler, 1983).

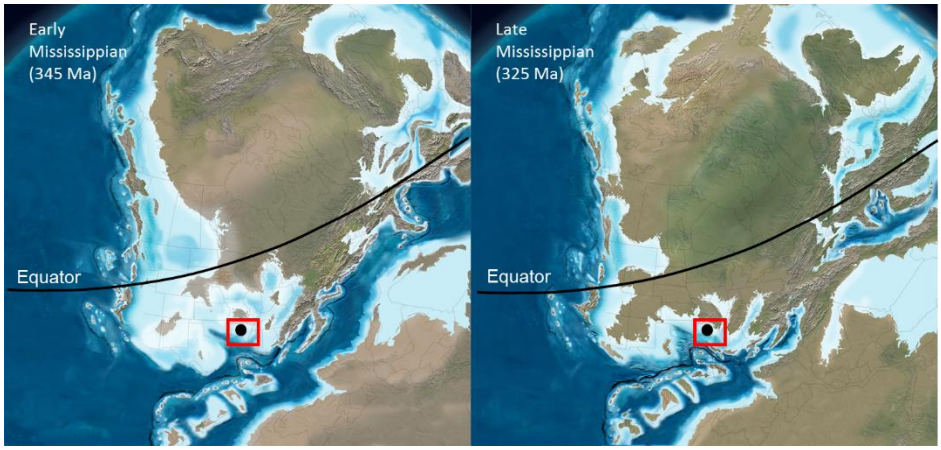

Figure 11. Paleogeographic maps during the Mississippian. Red box covers the state of Arkansas. Black dot indicates the general location of the study area (Blakey, 2008).

1. Paleoclimate

Paleoclimate conditions in the midcontinent region indicate an arid climate in the Mississippian that transitioned to a humid climate during the Pennsylvanian. The climate change is dictated by the midcontinent paleolatitude position, which drifted from the subequatorial zone into the equatorial zone illustrated by Figure 12 (Coleman, 2000). Precipitation was relatively low in the Mississippian. By the Pennsylvanian, precipitation significantly increased as sea level dropped and as continental convergence began. While precipitation was low, atmospheric conditions during the early Carboniferous have been reported to contain high concentration of $CO_{2,}$ (Borzenkova and Turchinovich, 2009), with carbon dioxide during the Phanerozoic reaching its maximum concentration in the Early Ordovician, Devonian, and Early Carboniferous. Atmospheric CO_2 gradually declined throughout the Carboniferous as vegetation flourished and absorbed CO_2.

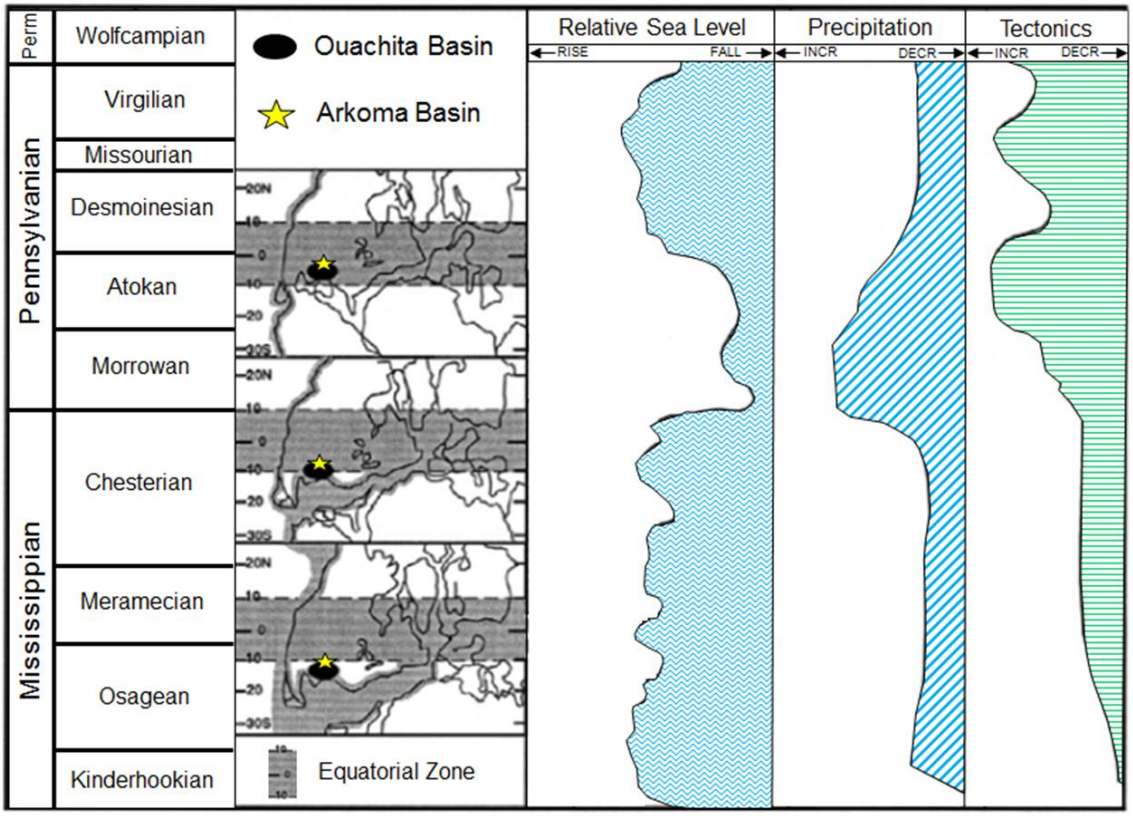

Figure 12. Paleogeographic position of the Ouachita Basin along with fluctuations of sea level, precipitation, and tectonic events during the Carboniferous. Modified from (Coleman, 2000).

2. Depositional Sequence

The Mississippian units are a part of a cratonic sequence known as the Kaskaskia cycle. The Kaskaskia cycle begins in the Middle Devonian and ends at the Mississippian-Pennsylvanian boundary. It is divided into two separate cycles as shown by Figure 13. The Mississippian lithostratigraphy is a component of Kaskaskia II. For approximately 3.6 million years, these units experienced rapid transgressions and regressions until transgressions slowed near the beginning of the Pennsylvanian (Manger, 2015). The Mississippian succession experienced twelve 4th order cycles during the Kaskaskia II sequence (Figure 13).

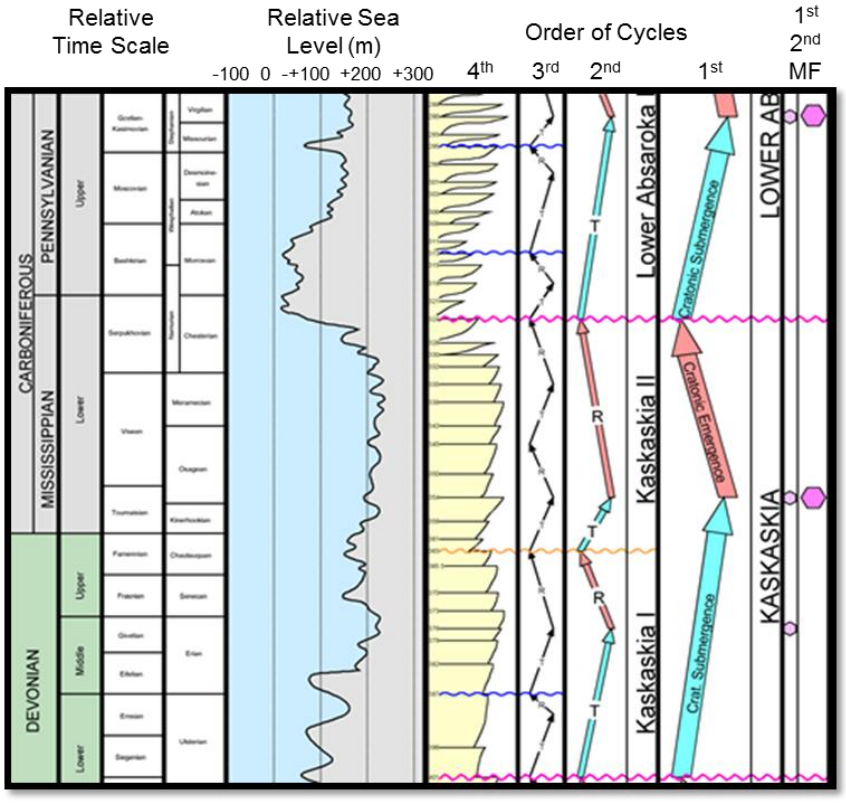

Figure 13. Relative sea level fluctuations during Devonian and Carboniferous (Manger, 2015).

The chert-bearing, Kinderhookian St. Joe-Osagean Boone Formations represent the oldest Mississippian strata in the eastern Arkoma Basin. The formations were deposited on a shallow ramp and adjacent Burlington Shelf, along the southern margin of North America during a highstand-regressive sequence. Following the deposition of the Boone Formation, the southern midcontinent region was exposed by a major fall in sea level. The Moorefield Shale was deposited as a wedge during these low-stand conditions in areas adjacent to the Mississippi Embayment to the east (Manger 2015). The Moorefield Shale in the subsurface of eastern Arkansas extends westward and pinches out in western Newton County, Arkansas. The Hindsville Limestone marks the initial transgressive system tract of the Chesterian Series. As sea level rose, the limestone was deposited across the shallow ramp. The Batesville Sandstone is the Hindsville Limestone lateral equivalent. It began progradation westward along the southern Ozark shelf from the northeast. As sea level continued to rise, the Hindsville-Batesville systems were drowned and covered with the Lower Fayetteville Shale. The black, pyritic, concretionary black shale represents a deeper, muddy, shelf environment. Micritic concretions reflect low sedimentation rates during early transgression (Manger 2015). Anoxic bottom conditions developed as sedimentation rates increased and created sideritic concretions during this maximum flooding. The Upper Fayetteville was deposited during the high-stand consisting of concretionary black shale on a storm-dominated, muddy shelf setting.

KARST SYSTEMS

A. Karst

The enclosed depressions observed on the Boone 3D seismic surface are interpreted here as paleokarst sinkholes. Ford and Williams (1989) describe karst as a "terrain with extensive underground water systems and landscapes that develop from highly soluble rocks and well developed secondary porosity." It is regarded as a "diagenetic facies" and is a process that affects sedimentation of carbonates (Esteban and Klappa, 1983). Examples of soluble rocks include limestone, dolomite, and gypsum. Enclosed eroded depressions are distinctive characteristics of these landscapes. They are formed over an extended period of time, as carbonic acid dissolves the host rock. Dissolution within the bedrock causes the surface to lower, weaken, and gradually collapse or subside. Typical geomorphic karst features include caves, depressions, sinkholes, dolines, and sinking streams.

Carbonates are deposited in a warm shallow marine environment and often experience multiple fluctuations of sea level. When sea level regresses and exposes the carbonate surface, the chances of dissolution increases as rainwater flows through the fractures and pores in limestones. As meteoric water flows through these cracks, they can open and enlarge the fractures and increase karst permeability. There are two hydrologic zones in the epikarst systems shown in Figure 14, where meteoric waters are capable of flowing: the vadose and the phreatic zones (James and Choquette, 1984). These zones are controlled by the water table. The vadose is the unsaturated zone above the water table closest to the surface. This zone experiences subaerial exposure and weathering of the karst unit. It is subdivided into the zone of infiltration and the zone of percolation. The

vertical, wavy lines within the vadose zone represent fractures or pore spaces that allows meteoric water to seep or percolate to the phreatic zone. The zone immediately above the water table is called the zone of capillarity flow. Once waters come in contact with this zone, saturation is disrupted because hydrostatic and atmospheric pressures are equal (Wright and Smart, 1994). Water then infiltrates the phreatic zone (saturated zone) where it diffuses laterally, developing multiple channels and filling pores spaces. Caves can also form in the phreatic zone in areas of higher fractured bedrock. The mixing zone blends the meteoric and saline water to create brackish water.

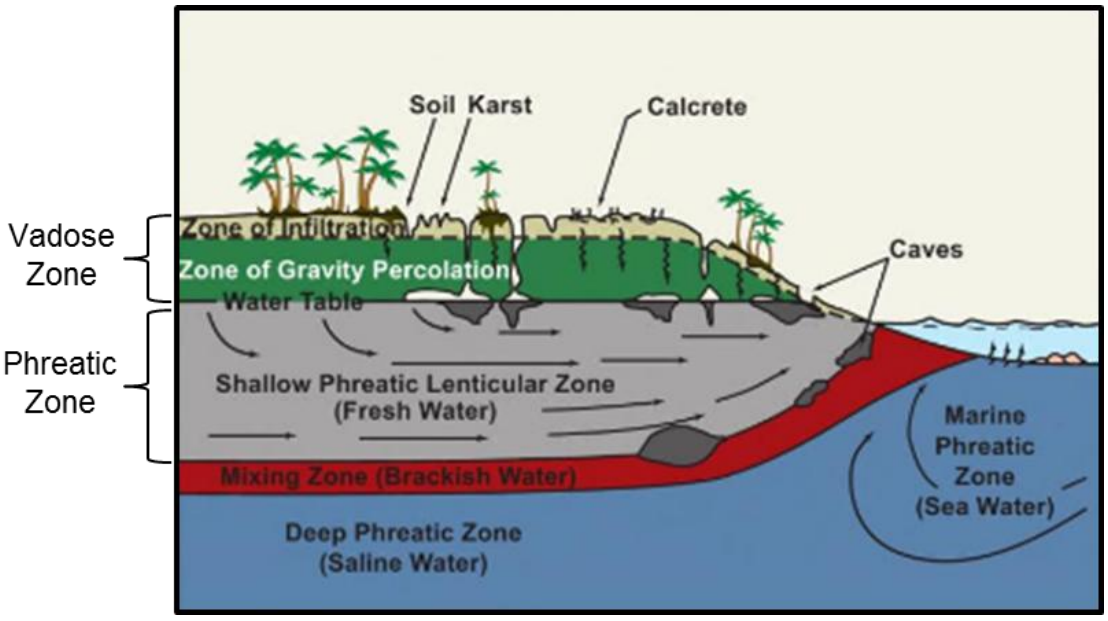

Figure 14. Systematic profile showing the hydrological zones present in a meteoric domain. Modified from (Scholle and Ulmer-Scholle, 2003).

Soluble rocks in the study area are primarily limestone. Diagenesis of these rocks can occur immediately upon exposure and contact with meteoric water. Carbonic acid is the primary source for dissolution (Wright and Smart, 1994). It is created through the mixing of atmospheric or soil carbon dioxide and rainwater through the equation below (Boggs, 2012, p. 7).

$$CO_2 + H_2O = H_2CO_3 = H^+ + HCO^-_3$$

Because limestones have a very low solubility rate with pure water, the driving factor for dissolution is carbon dioxide within biogenic material (Waltham *et al*., 2005). Meteoric water picks up a very small amount of carbon dioxide content as it falls through the atmosphere. The source for most of the carbon dioxide is derived from the oxidation of organic matter within the soils. When organic material decays, it releases major amounts of carbon dioxide content that percolates through the soil into solution by rainwater (Waltham *et al*., 2005). If biogenic concentrations of carbon dioxide are relatively high, it only takes a small amount of precipitation to dissolve the bedrock. The dissolution rates in limestone depend on latitude and precipitation. Meteoric diagenesis is best utilized in tropical regions with humid temperatures. Dissolution of carbonates increase with warmer temperatures because it promotes the oxidation of organic material (Moore and Wade, 2013, p. 170). Since diagenesis is dependent upon meteoric waters, increased rainfall will increase the dissolution process.

B. Dolines

As rainwater continues to flow through the permeable layer, the ground is susceptible to fracture-enhanced dissolution that creates the downward closed depressions. After the ground surface is lowered, it is further prone to subsidence or collapse. These distorted features are known as sinkholes or dolines. Sinkhole is a term that is more widely used in the North American literature. Geomorphologist use the term doline because there is a minor confusion on what constitutes a sinkhole or a depression (Waltham *et al*., 2005). There are six main types of dolines classified by formation process and scale (Figure 15). Dolines have a shape that is typically circular or bowl shaped, and vary in diameter and depth. Each doline results from dissolution in the bedrock and fissure enlargement. They differ in their failure mechanisms and host rock, which gives them a unique structure and gradient profile. A common rock that is frequently associated with sinkholes is breccia. Breccia is formed by cave or sinkhole collapse and subsequent cementation and compaction of the bedrock fragments. Large-scale collapse breccia can be recognized in 3D seismic data as an amplitude anomaly created by the acoustic impedance (AI) contrast between host limestone (high AI) and breccia (low AI). In chert-bearing limestones such as the Boone, insoluble chert remnants are likely to accumulate at the bottom of a sinkhole.

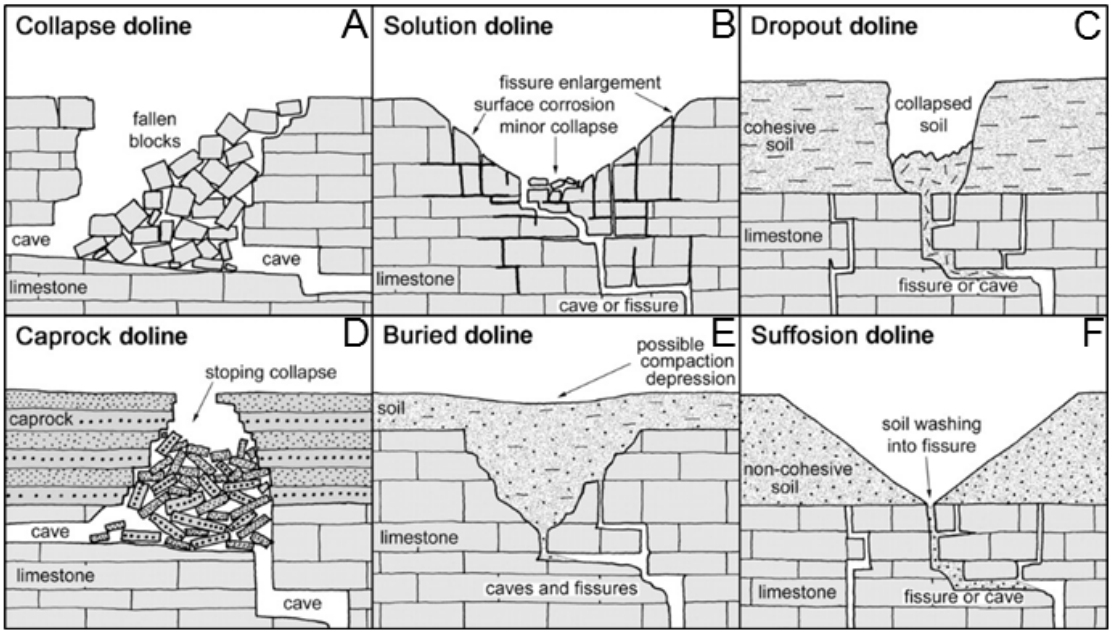

Dolines	Formation process	Host rock types	Typical max size
Collpase	Roof failure	Limestone, dolomite, gypsum, basalt	Up to 300 m across Up to 100 m deep
Solution	Dissolutional lowering of surface	Limestone, dolomite, gypsum, salt	Up to 1000 m across Up to 100 m deep
Dropout	Soil collapse	Cohesive soil overlying carbonates	Up to 50 m across Up to 10 m deep
Caprock	Failure of insoluble rock	Rocks overlying limestone, dolomite, and gypsum	Up to 300 m across Up to 100 m deep
Buried	Soil filled after environmental change	Rockhead depressions in carbonates	Up to 300 m across Up to 100 m deep
Suffosion	Downwashing of soil	Non-cohesive soil over carbonates	Up to 50 m across Up to 10 m deep

Figure 15. Cross section of the six main types of sinkholes with their formation process, host rock types, and typical max size. Modified from (Waltham *et al*., 2005).

C. Paleokarst

Ford and Williams (1989) define paleokarst as "karst features that formed in the past and are buried by younger sediments and are hydrologically dissociated from the contemporary system". Subsurface paleokarst was not well understood until the 1990s, when 3D seismic data made it possible to identify paleokarst features. However, paleokarst structure and geometry are still research areas. Present day karst systems aid to the understanding of ancient and inactive karst features in the subsurface (Wright and Smart, 1994). Paleokarst contributes to the earth's geological history by revealing major and minor unconformity events. Hydrocarbon exploration has led to enhanced research on paleokarst features through seismic and borehole data (Wright and Smart, 1994). These features can be hydrocarbon reservoirs due to significant increased porosity in carbonate rocks or by forming stratigraphic traps that limit the migration of hydrocarbons (Maslyn, 1997).

Paleokarst surfaces formed in the past when sea level dropped to expose carbonate rock units. There are two major unconformities identified in the U.S. midcontinent that relate to possible development of paleokarst surfaces: Sauk sequence (Early/Middle Ordovician) and the Kaskaskia sequence (mid-Carboniferous) (Palmer and Palmer, 1989). As shown in Figure 13, the Mississippian carbonate rocks in this study fall within the Kaskaskia II sequence. Figure 16 is a map of the United States that highlights the distribution of karst areas during this time (Palmer and Palmer, 1989). The northern half of Arkansas is included in this section and indicates that paleokarst features could be present in the study area. Areas not highlighted are generally clastic rocks not prone to karsting. However, karst features are not limited to these two major

unconformities. Palmer and Palmer (1989) note that the earliest karst episode during the Carboniferous occurred at the end of the Osagean Epoch (Boone/Moorefield). The Osagean/Meramecian unconformity developed due to minor subaerial exposure in carbonates that created dolines and small caves that were filled with Meramecian sediments (Palmer and Palmer, 1989). This statement is important because it supports the possibility of paleokarst features, such as sinkholes, occurring in the Boone limestone. Paleokarst are also a common feature in foreland basins (Wright and Smart, 1994). Uplift along the thrust belt and vertical loading causes flexural downwarping within the foreland basin. Consequently, formations within the basin get uplifted and are potentially exposed to karsting.

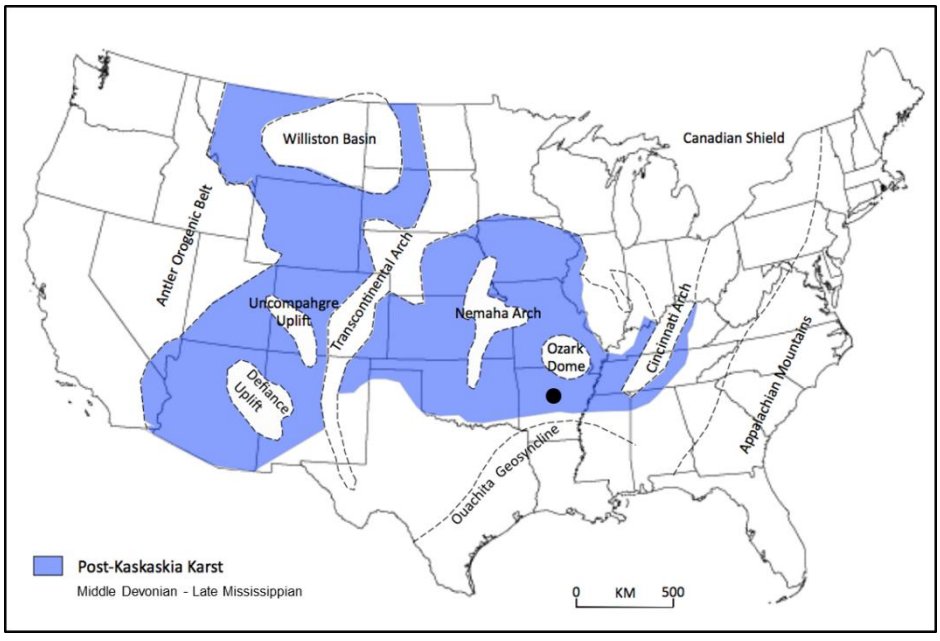

Figure 16. Paleogeographic setting of the post-Kaskaskia erosional events that shows the location of karst surfaces in the United States. Black dot denotes the study area. Modified from (Palmer and Palmer, 1989).

DATA DESCRIPTION

Southwestern Energy (SWN) donated the 9 sq. mi. Desoto 3D seismic survey located in the northeast corner of Conway County, Arkansas displayed in Figure 2. The survey was acquired and processed in 2010 by GXTechnology (ION Solutions) using pre-stack time migration. The survey parameters are listed in Table 1. Desoto has a bin size of 110 x 110 feet, datum of +500 SS, time sample rate of 2 milliseconds and trace length of 2 seconds. The survey contains 145 inlines with a range of 11150-11295 (North-South) and 145 crosslines with a range of 1585-1730 (East-West). The Desoto Survey was uploaded into OpendTect, an open source seismic software system used for interpreting and visualizing multi-volume seismic data. Additionally, SWN provided acoustic impedance (AI) and vp/vs (VPVS) attribute volumes along with well, production and geosteering data. AI and VPVS aid in understanding rock properties associated with stratigraphic units. Geosteering data was not used in this study, but can be useful in future work.

SWN also provided LAS (digital wireline log) files for the wells drilled in the study area shown in Figure 17. The current study used only one well in the survey (Bryant Coy), denoted by the green dot in Figure 17. The remaining wells did not penetrate through all of the Mississippian formations, targeting the Lower Fayetteville shale formation and landing above the Boone limestone. The Bryant Coy well had a digital sonic log, important in seismic interpretation in order to correlate geological formations with their respective 3D seismic horizons. Bryant Coy sits at an elevation of 865 feet and has a total measured depth of 4,398 feet. The surface coordinates for this well are located at a latitude of 35.435239° and longitude of -92.523355°. The LAS file

for Bryant Coy included gamma ray, density, and sonic logs. Formation tops in Bryant Coy begin with the Lower Pennsylvanian Sells and end with the Lower Mississippian Boone Limestone.

Dominant frequency was estimated from a frequency spectrum calculated in OpendTect (Figure 18). The frequency spectrum ranges from 8-98 Hz (at 20dB down), which results in a dominant frequency of 53 Hz. Average velocity to top Boone was calculated from (Liner, 2004):

$$V_{avg} = 2 * (MD - KB + SRD) / T$$

where MD is measured depth, KB is kelly bushing, SRD is seismic reference datum, and T is reflection time. Inserting values for the Boone in the Bryant Coy well and the Desoto seismic survey yields:

$$V_{avg} = 2 * (3938ft - 865ft + 500ft) / (0.616sec) = 11{,}600 \text{ ft/s}$$

This value is important for time-depth conversion of the Boone 3D seismic horizon. The average interval velocity was used to calculate the Boone wavelength:

$$\lambda = V_{int}/f_{dom}$$

$$\lambda = 19{,}000 \text{ ft/s}/53 \text{ Hz}$$

This yields a value of 359 ft for the wavelength, then vertical resolution and lateral resolution as:

$$\text{Vertical Resolution} = \lambda/4 = 90 \text{ ft}$$

$$\text{Lateral Resolution} = \lambda/2 = 179 \text{ ft}$$

Vertical and lateral resolution measure how large a feature needs to be in order to be detected in seismic. Any object less than the resolution cannot be distinctly seen in the seismic data.

Survey Parameters	
Area	9 Sq Miles
Bin Size	110 ft x 110 ft
Crossline Range	1585 - 1730 (West - East)
Inline Range	11150 - 11295 (South - North)
Survey Reference Datum	500 ft above sea level
Time Sample Rate	2 msec
Trace Length	2 sec
Frequency Range	8-98 Hz
Dominant Frequency	53 Hz
Average Velocity (Boone)	11,600 ft/s
Interval Velocity (Boone)	19,000 ft/s
Wavelength (Boone)	359 ft
Vertical Resolution (Boone)	90 ft
Lateral Resolution (Boone)	179 ft

Table 1. Survey parameters for the Desoto Survey

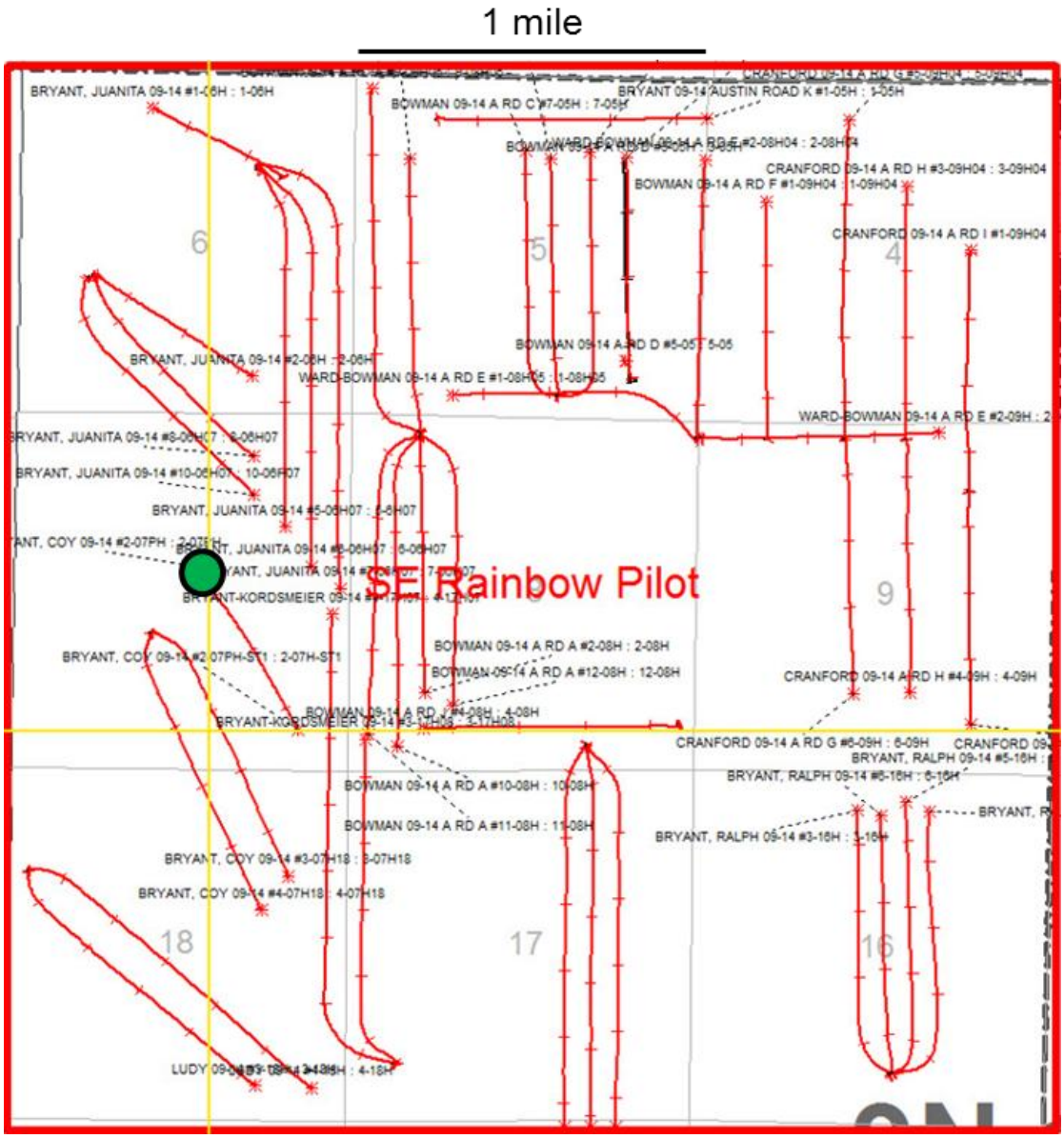

Figure 17. Higher magnification view of the survey area displaying all of the wells provided by Southwestern Energy. The green dot marks the location for the well used in this study.

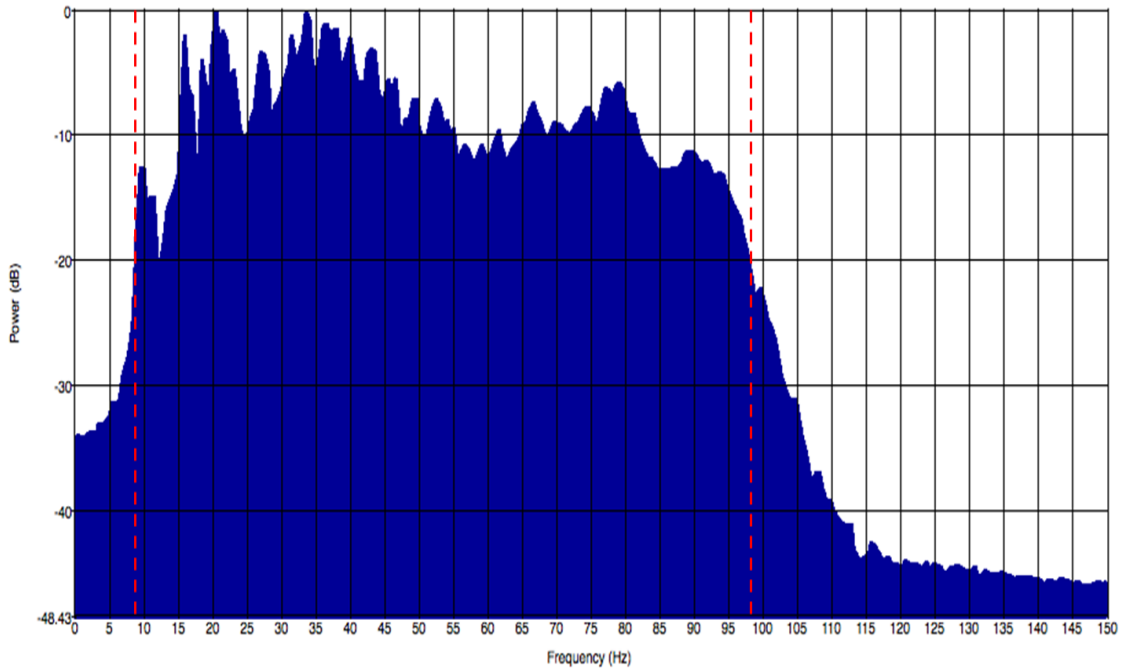

Figure 18. Frequency spectrum histogram from OpendTect of the Desoto Survey.

METHODS OF INVESTIGATION

A. Well Log Correlations

The first step for this research was correlating the well formation tops and seismic horizons. The synthetic seismogram was created using SeismicUnix (Figure 20a). Sonic and density logs from the Bryant Coy well were imported, velocity in ft/s was calculated by 1,000,000/sonic, and acoustic impedance (AI) at every depth level was formed by velocity x density. The AI depth log was stretched to time using the sonic velocities. After calculating the acoustic impedance, the reflection coefficients were calculated and filtered to the field data bandwidth. A plot for each of these logs were generated and placed side by side to compare and correlate the formation tops (Figure 19). The main logs that were used for correlation purposes were the gamma ray and acoustic impedance. The formation tops were picked on the gamma ray and acoustic impedance based on depth and visually correlated into the AI time plot and thus into the Desoto field data. Bryant Coy well logs were also uploaded into OpendTect for direct display on the seismic data. Figure 20b shows the Bryant Coy well tie and formation tops.

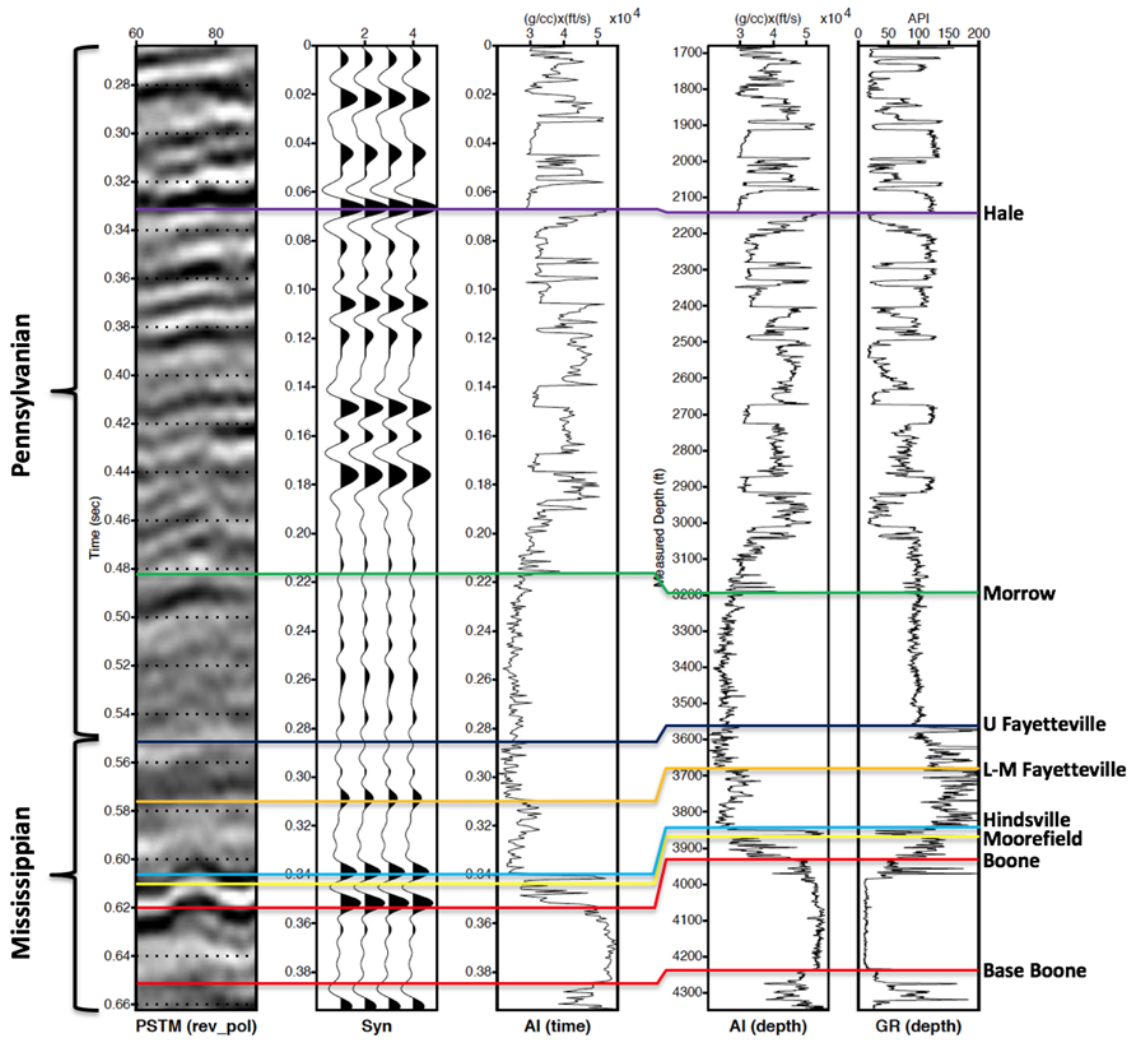

Figure 19. Cross section denoting the correlation of the stratigraphic units from Bryant Coy 09-14 #02-07PH. From left to right, the logs displayed are: Pre-stack time migration lines, Synthetic Seismogram, Acoustic Impedance in time and in depth, and Gamma Ray. (C. Liner, 2016, personal communication)

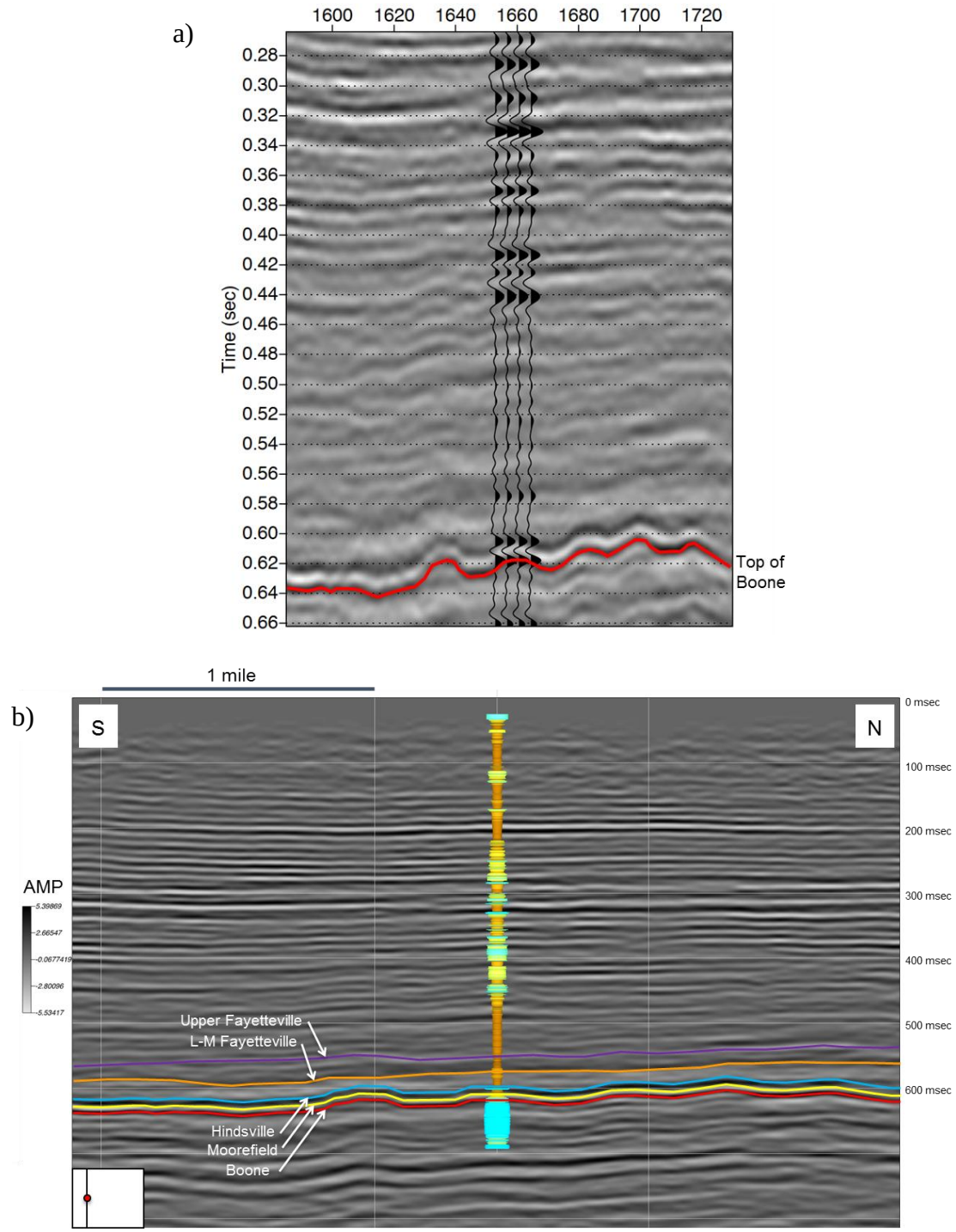

Figure 20. (a) Synthetic seismogram trace on inline 11178. (C. Liner, 2016, personal communication). (b) Bryant Coy well with velocity log displayed in seismic Inline 11178 with formation tops. The lower left corner shows the base map with the location of the seismic line and well within the survey. Well log display is velocity (color and deflection).

B. Horizon Tracking

Seismic event horizons were tracked from oldest (Boone Limestone) to youngest (Upper Fayetteville Shale). The Hindsville, Moorefield, and Boone horizons are very continuous throughout the seismic survey. In two areas, they are offset by minor normal faults that were first tracked in the survey before tracking the horizons. Figure 21 shows a zoomed image of faults (A and B) offsetting the Boone, Moorefield, and Hindsville. Offsets for the faults were estimated by finding the time for a horizon adjacent to each side of the fault, converting the time into depth, and subtracting the difference. Throw for both faults at Boone level is about 60 ft. The faults strike east-west and dip southward, which are consistent with Van Arsdale and Schweig (1990) faults closest to the study area.

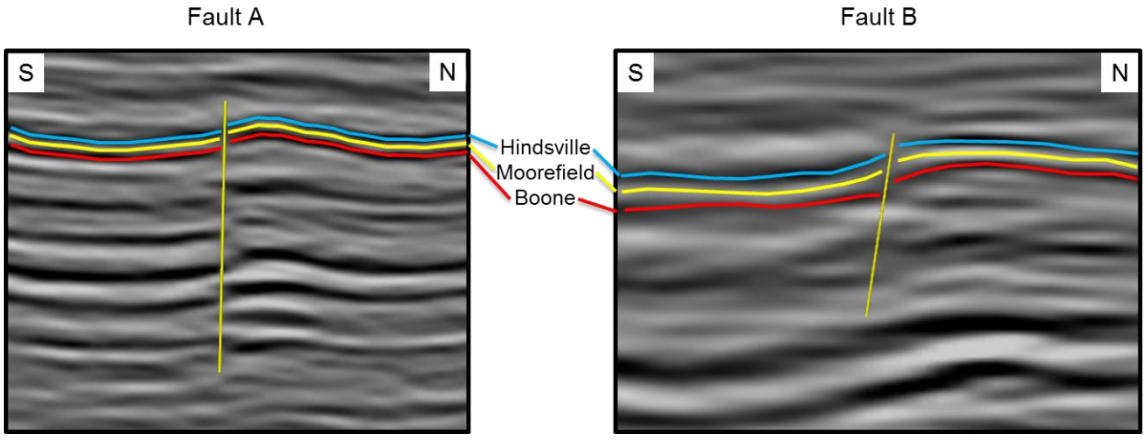

Figure 21. Fault A is located on inline 11173. Fault B is located on inline 11289.

Boone, Moorefield, and Hindsville horizons were picked on inlines and crosslines across the entire survey. After picking these events, they were auto-tracked and extrapolated through the survey to result in a continuous time structure map. Figure 22 shows the time structure map of the Boone Formation. Hot colors represent shallow areas and cool colors represent deep. The closed contour lines within structural lows are interpreted as paleokarst sinkholes in the Boone Limestone.

The Lower-Middle Fayetteville marks an unconformity in the survey which makes it difficult to auto-track. The Upper Fayetteville was also very difficult to auto-track because it contains a weak amplitude (shale-on-shale contact) and inconsistent geology. Instead of auto-tracking, these surfaces were manually tracked. Horizons were manually picked on every 10^{th} line to make a cloud point and were gridded to construct a time structure map. To reduce noise acquired from gridding, the maps were then smoothed. After the time structure maps were generated, a 4 msec contour overlay was added.

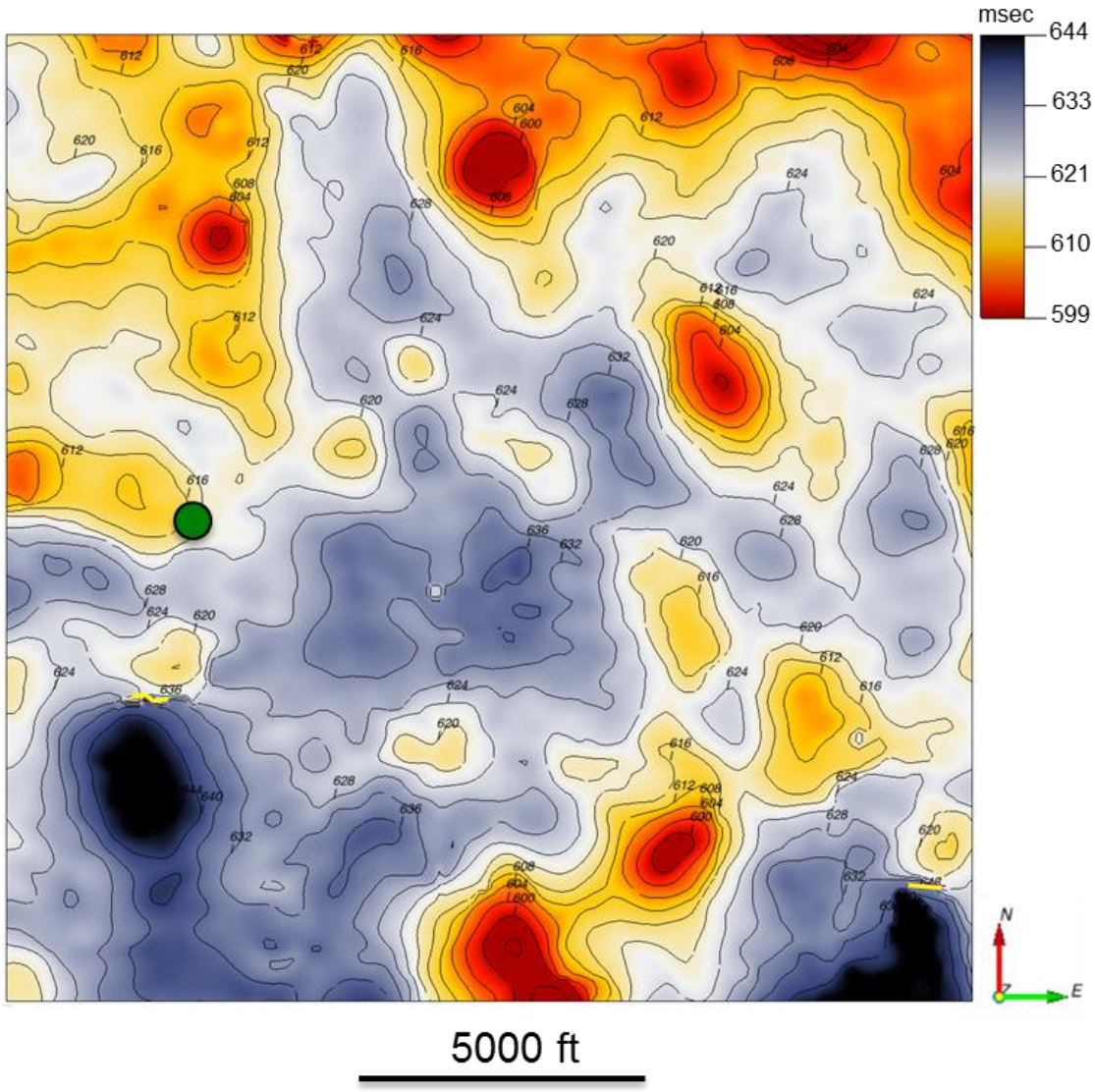

Figure 22. Time structure map of the Boone Formation with 4 msec contour intervals. The green dot denotes the Bryant Coy well location.

C. Time-Depth Conversion

Converting the time structure maps to depth was essential to visualize the maps in a depth perspective. The first step was calculating the average velocity for each formation. An example of this calculation is shown for the Boone Formation in the data description. The same procedure was applied to the rest of the Mississippian units with the parameters listed in Table 2. Half the average velocity multiplied by reflection time was subtracted from the seismic reference datum to estimate true vertical depth subsea (TVDSS) using the equation:

$$TVDSS = SRD - (V_{avg} \times T/2)$$

TVDSS and T are grids, where SRD and V_{avg} are constants. This equation was implemented in OpendTect to generate a depth structure map. A contour overlay was then added with an interval of 20 ft. The depth structure map for the Boone Formation is displayed in Figure 23.

Formations	Time (sec)	MD (ft)	Vavg (ft/s)
Boone	0.601	3938	11601
Moorefield	0.604	3866	11593
Hindsville	0.600	3850	11617
L-M Fayetteville	0.530	3684	12525
U Fayetteville	0.555	3565	11636

Table 2. Formation tops for the Mississippian units with their average velocity.

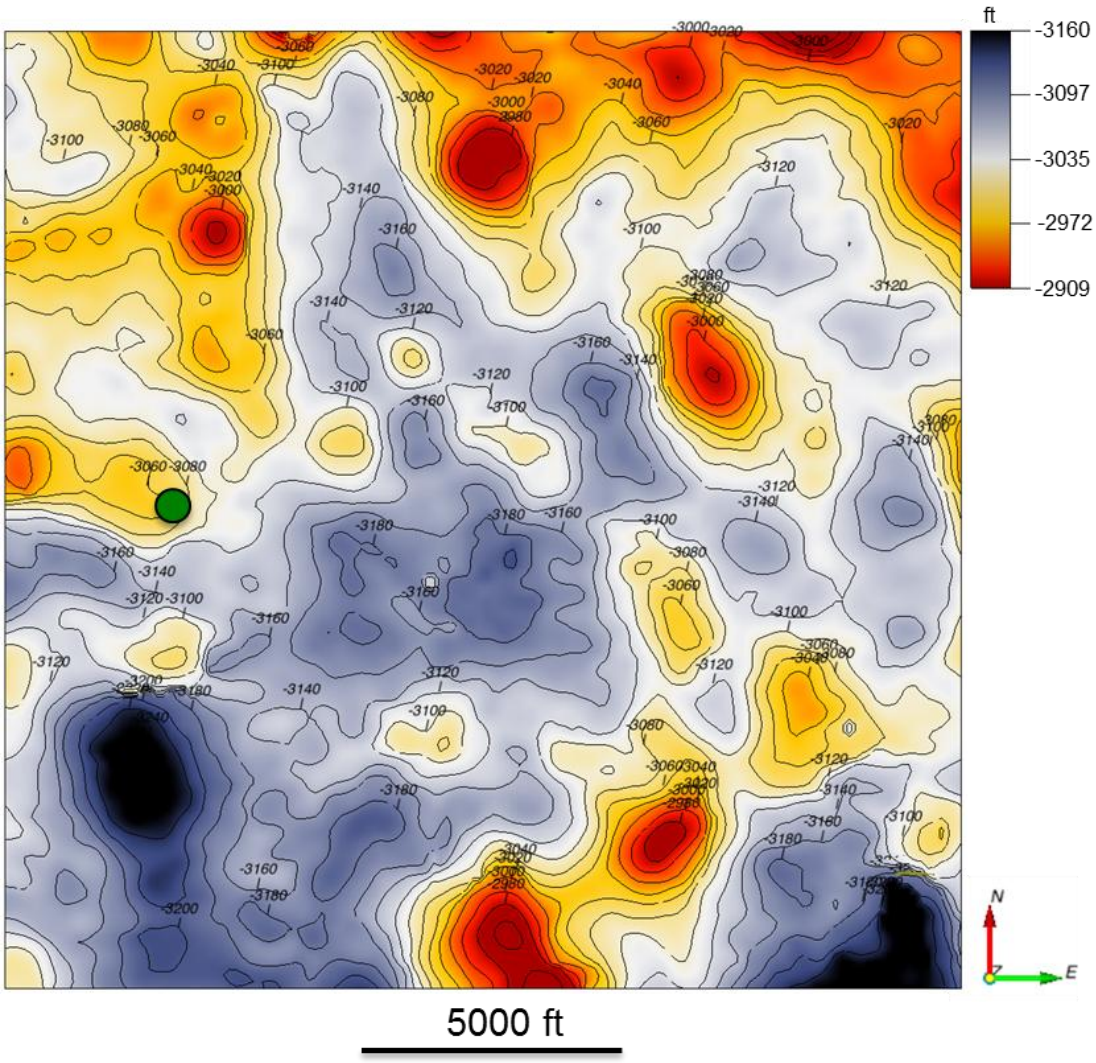

Figure 23. Depth (TVDSS) structure map of the Boone Formation with 20 ft contour intervals.

D. Sinkhole Measurements

Paleokarst sinkholes are recognized as having a circular or oval shape and most specifically, enclosed depressions. Sinkholes were identified on the Boone 3D seismic horizon (time structure map) based on these characteristics. Depressions in the time structure map that show closed contour lines are accepted as sinkholes. Evidence of 14 sinkholes was mapped and numbered as a point in the survey area. There were some potential sinkholes along survey edges not included in this count, since they were incompletely imaged (*e.g.*, the depression in the bottom right corner of Figure 22).

The dimensions for all 14 sinkholes were analyzed in an open source software called ImageJ, an image processing program for scientific analysis. A gray scale image of the structure map for the Boone Formation was captured and uploaded into ImageJ. The first step was to calibrate the image by making a scale of 3 miles across the survey. To keep the units consistent, miles was converted into feet to give an area of the survey of 15840 x 15840 ft. Once the image was to scale, the threshold was adjusted for each individual sinkhole. The threshold separates pixels that fall within a desired range of intensity values. While adjusting the threshold, each sinkhole is defined by its largest closed contour. An example for the first sinkhole is shown in Figure 24. Once the threshold was adjusted to capture the full size of the sinkhole, the figure was traced and outlined, analyzed, and measured by ImageJ.

ImageJ measurement parameters are set by the user to return particular aspects, such as area, shape descriptors, perimeter, etc. The same procedure was applied to all 14 sinkholes. The depth of the sinkholes cannot be measured by using ImageJ. To determine the depth of the sinkholes, I calculated the average of the interval velocity from the base

of the Lower Fayetteville to the top of the Boone. This interval velocity of 12,025 ft/s was used to estimate the depth for the sinkholes. The depth of each sinkhole was determined by finding the difference between the highest and lowest contour line that enclosed the depressions. Figure 25 shows the 14 assigned sinkholes and the results of the sinkhole measurements. For a description of the measurement parameters defined by ImageJ, refer to the appendix.

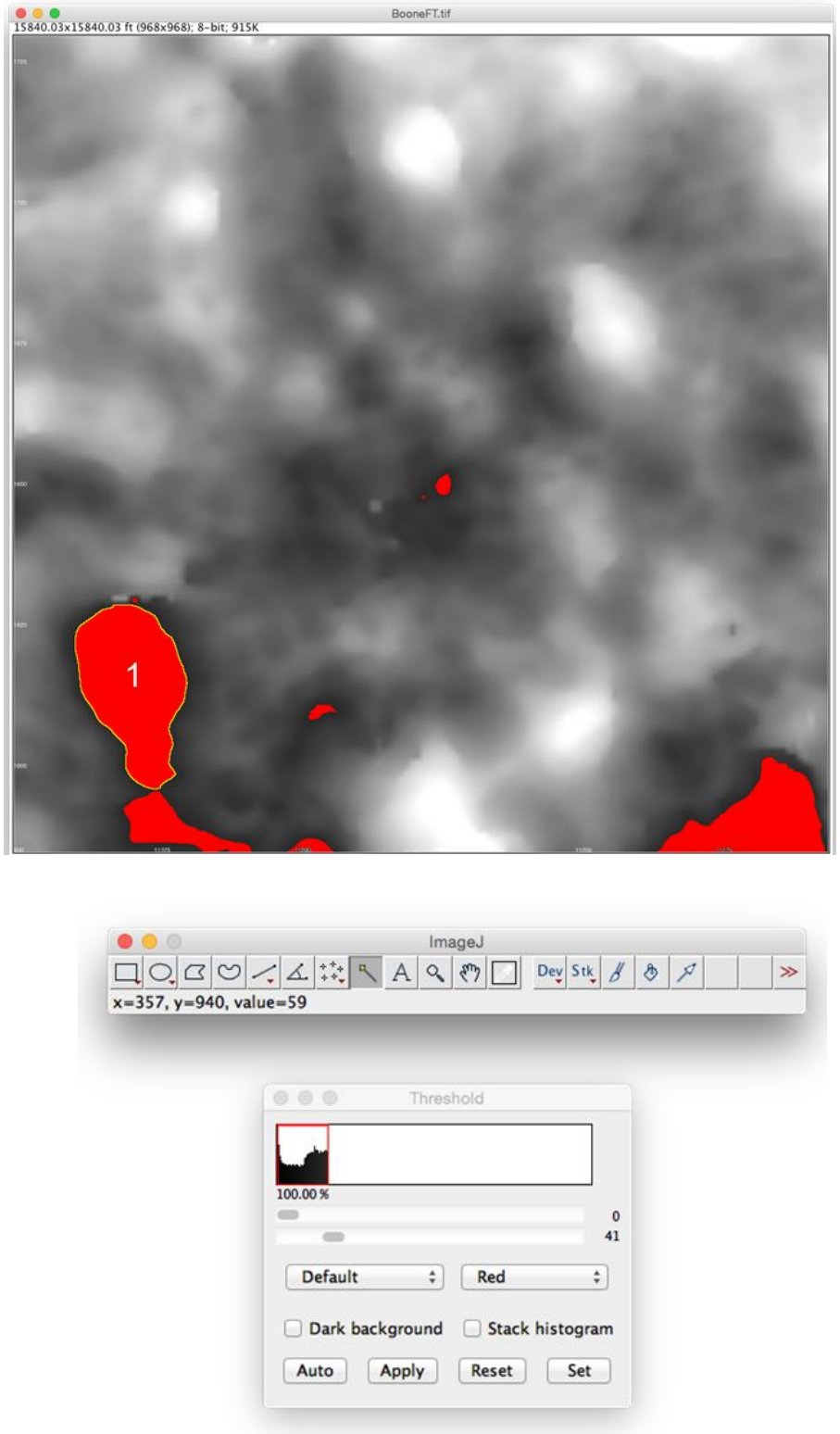

Figure 24. Gray scale image of the Boone structure map uploaded into ImageJ. To the right is an image of the threshold function isolating Sinkhole #1.

Results

	Area	Min	Max	X	Y	Perim.	Major	Minor	Angle	Circ.	Feret	FeretX	FeretY	FeretAngle	MinFeret	AR	Round	Solidity
1	5076643.254	0	41	2320.508	12598.469	9836.641	3488.009	1853.144	104.900	0.659	3671.191	1930.913	11029.111	103.665	2027.989	1.882	0.531	0.920
2	1186754.729	39	57	5787.698	13442.047	5228.267	1979.550	763.316	49.278	0.546	2019.836	5138.191	14334.572	49.600	916.396	2.593	0.386	0.835
3	1845467.868	51	62	5850.673	9269.858	8694.474	2083.232	1127.922	86.267	0.307	2233.206	5383.646	8263.651	118.443	1533.614	1.847	0.541	0.641
4	2815061.476	33	62	8088.939	9210.275	8527.830	2176.860	1646.522	79.275	0.486	2480.809	7281.831	10292.746	53.584	1962.819	1.322	0.756	0.782
5	778138.367	65	86	6855.836	6803.062	3573.975	1263.500	784.137	112.246	0.766	1285.355	6627.285	6218.193	121.464	791.928	1.611	0.621	0.941
6	2706347.031	62	98	6408.733	3929.913	7786.332	2299.147	1498.742	123.365	0.561	2855.401	6021.829	2700.005	124.965	1768.681	1.534	0.652	0.854
7	3268930.895	49	89	9947.700	6519.190	8665.036	2942.518	1414.480	111.859	0.547	2942.276	9212.744	5285.464	127.316	1608.829	2.080	0.481	0.798
8	2287287.656	84	116	12666.725	3580.365	6965.823	1752.682	1661.605	140.958	0.592	2211.276	11601.839	3763.643	177.455	1867.591	1.055	0.948	0.819
9	1288507.165	99	115	14344.559	4940.450	5271.543	1534.389	1069.206	7.108	0.583	1937.074	13483.661	4876.373	8.746	1141.415	1.435	0.697	0.840
10	1874922.520	67	99	14691.160	7796.020	5589.912	1836.197	1300.092	85.244	0.754	1990.726	14514.572	8721.834	80.538	1398.621	1.412	0.708	0.944
11	1558954.429	81	105	12360.206	8463.388	4936.329	1746.053	1136.806	141.657	0.804	1801.862	11667.294	7805.469	140.528	1208.143	1.536	0.651	0.965
12	463509.124	84	102	14871.533	9893.623	2618.586	794.605	742.706	161.515	0.849	871.125	14498.208	9638.199	151.991	750.583	1.070	0.935	0.962
13	985392.013	108	124	11802.548	11080.834	4300.954	1348.223	930.588	84.514	0.669	1509.188	11880.022	11781.840	80.640	1058.824	1.449	0.690	0.903
14	824462.502	50	64	13093.056	14063.535	3685.713	1146.561	915.554	104.809	0.763	1230.217	12632.750	13647.298	118.610	1012.296	1.252	0.799	0.948

Results Table

Sinkholes	Depth
1	60 ft
2	18 ft
3	30 ft
4	54 ft
5	18 ft
6	36 ft
7	36 ft
8	36 ft
9	18 ft
10	30 ft
11	24 ft
12	24 ft
13	18 ft
14	18 ft

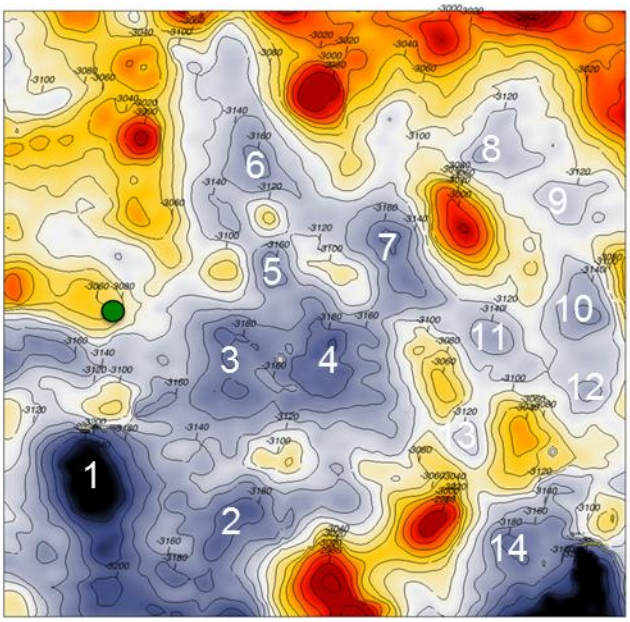

Boone Depth Map

Figure 25. Sinkhole measurement results with reference numbers for the Boone. Contour interval = 20 ft.

RESULTS AND OBSERVATIONS

A. Structure Maps

Time and depth structure maps for Moorefield, Hindsville, Lower-Middle Fayetteville, and Upper Fayetteville are displayed in Figures 26-29. They are in stratigraphic order from the oldest to the youngest formation. Structural patterns for the Boone, Moorefield, and Hindsville surface are very similar, all show sinkhole topography, are offset by the two minor faults, and contain the same general slope. The 14 sinkholes are approximately the same shape and size in all three maps. I interpret this to imply that sinkholes in the Boone Limestone controlled the landscape morphology for the Moorefield Shale and Hindsville Limestone. The Hindsville is slightly different in the area around sinkhole 3 and 4 due to stratigraphic terminations in the horizon, perhaps caused by Hindsville dissolution.

By the Lower-Middle Fayetteville, the structure had significantly changed. All of the sinkholes were completely filled, except for the possible remnant of two sinkholes in the center and southwest corner of the area. Upper Fayetteville shows no sinkhole topography. Taken together, these results support the interpretation of paleokarst and sinkhole development in the Boone that continued through the Moorefield and Hindsville time with probable local dissolution thinning of the Hindsville. Later deposition of Fayetteville Shale infilled the sinkhole terrain and marked the end of karst development.

Strike and dip orientation for the faults are consistent with Van Arsdale and Schweig (1990), see Figure 7. The structural high is north-northeast and sloping downwards toward the southwest section of the area. The gradient is more apparent in the Fayetteville Shale maps. In the Boone, Moorefield, and Hindsville maps, the landscape is

covered by conical hills and doline features. Most of the mound features are scattered towards the north and southeast section of the map that represent general structural highs. Sinkholes are located within this barrier trending northeast to southwest. It is also apparent that every sinkhole is adjacent or surrounded by a mound which is characteristic of a cockpit karst landscape (Waltham *et al*., 2005).

An isopach map was made to show true stratigraphic thickness from the top of the Upper Fayetteville Shale to the top of the Boone Limestone (Figure 30). The color bar shows the thin areas as dark blue, gradually thickening through lighter colors with the thickest areas in red. The isopach shows stratigraphic thickening toward the east. The thickest section in this area is segregated by north-south trending contour lines influenced by paleotopography of the Boone surface. Closed contours on the isopach map are associated with the mounds and sinkholes in the Boone, Moorefield, and Hindsville topography. Thinning on the east boundary of the isopach map may be edge effect artifacts or indicate true thinning. An arbitrary line was taken from the isopach map that intersects the thinnest and thickest sections. The cross-section is shown in Figure 31.

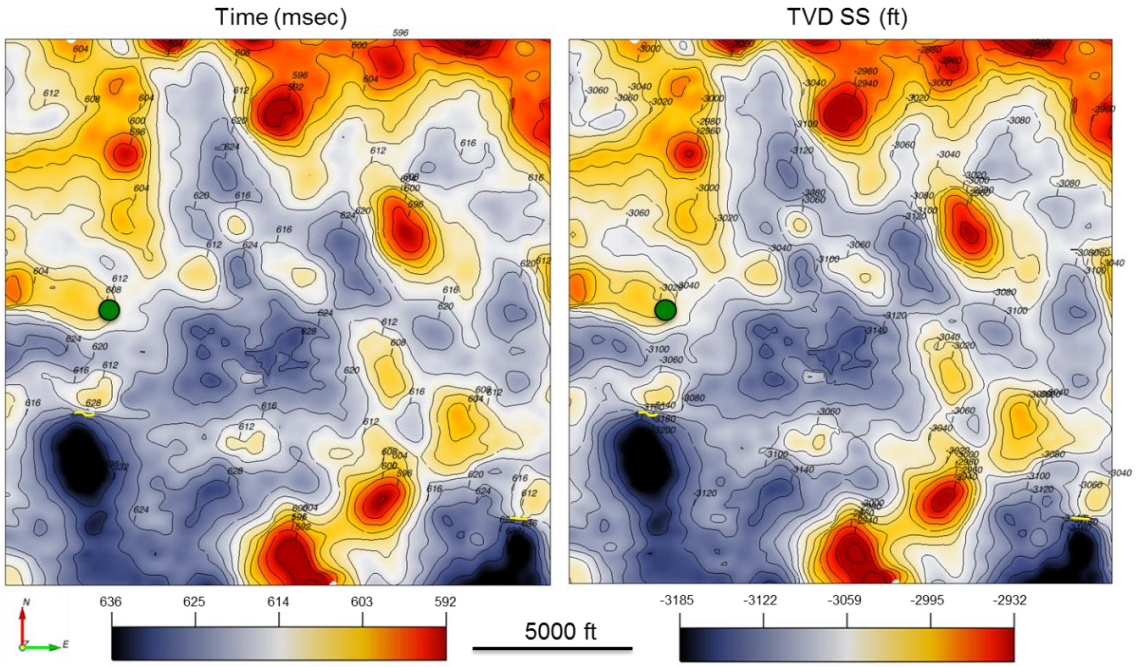

Figure 26. Time and depth structure map of the Moorefield. (Left) Contour interval = 4 msec. (Right) Contour interval = 20 ft.

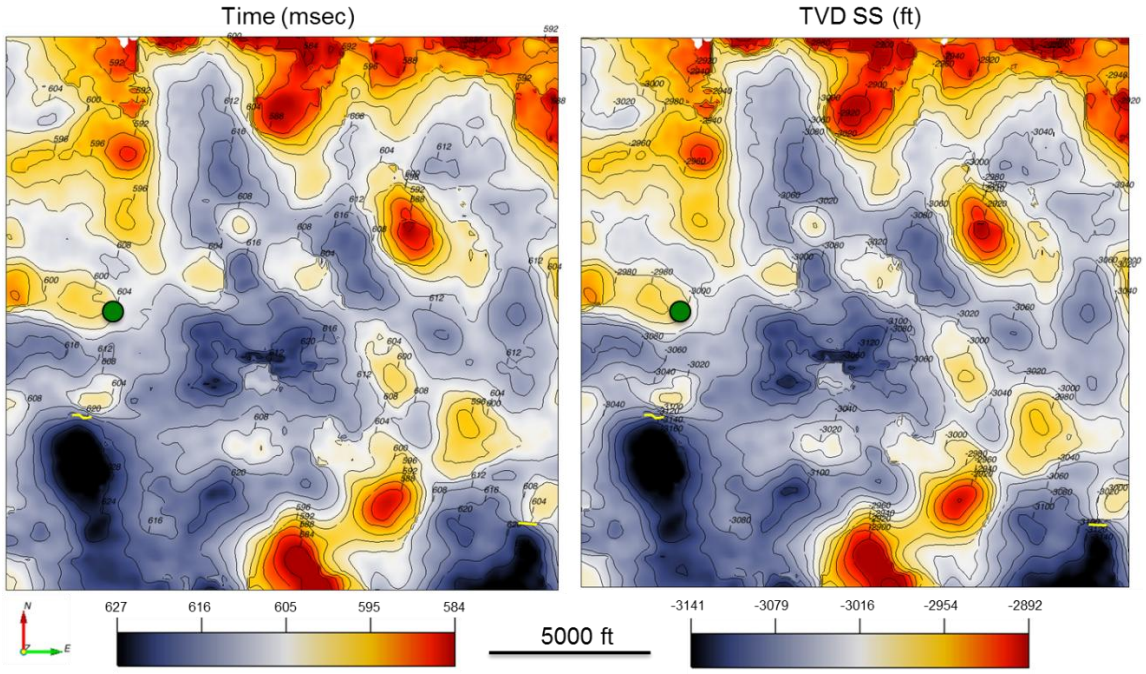

Figure 27. Time and depth structure map of the Hindsville. (Left) Contour interval = 4 msec. (Right) Contour interval = 20 ft.

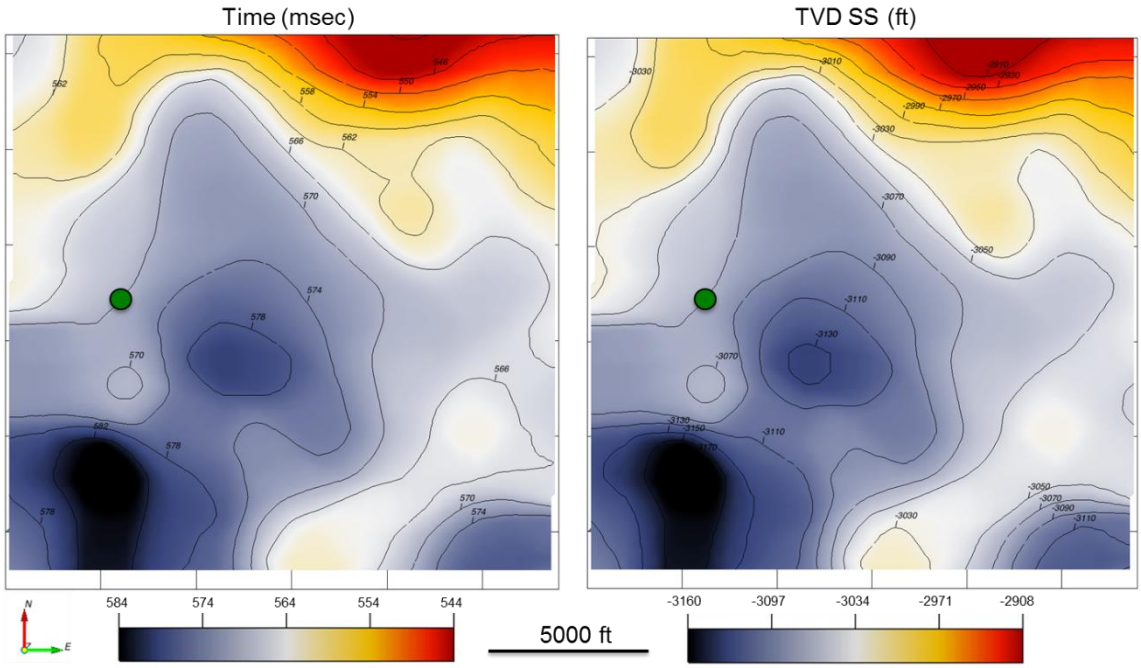

Figure 28. Time and depth structure map of the Lower to Middle Fayetteville. (Left) Contour interval = 4 msec. (Right) Contour interval = 20 ft.

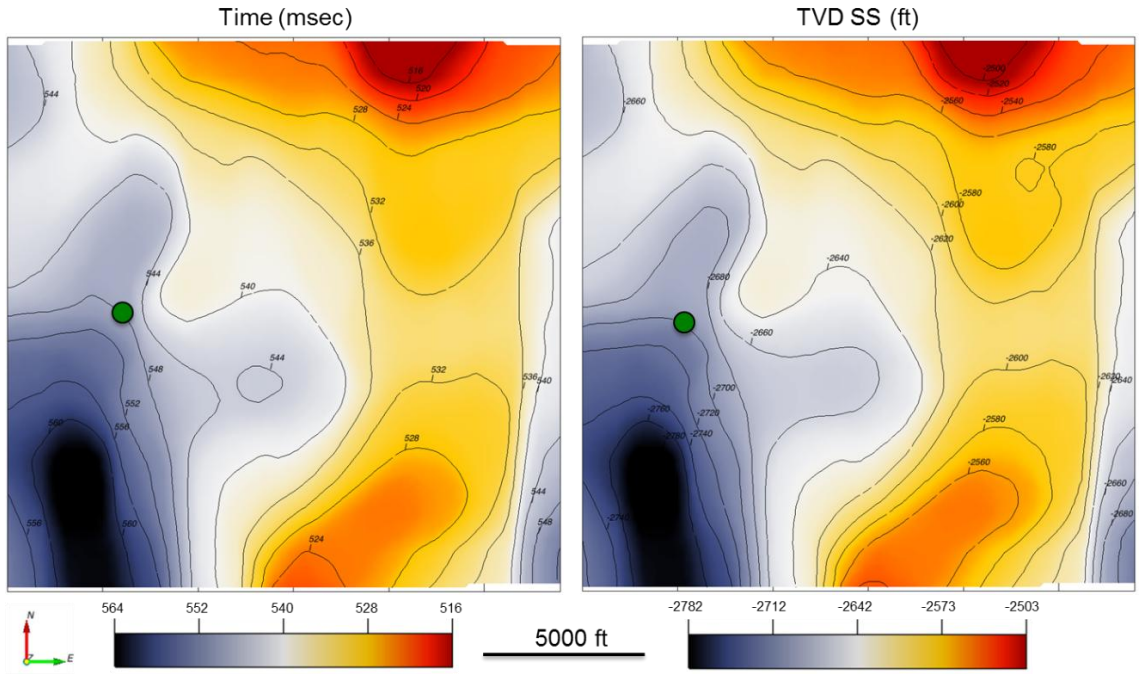

Figure 29. Time and depth structure map of the Upper Fayetteville. (Left) Contour interval = 4 msec. (Right) Contour interval = 20 ft.

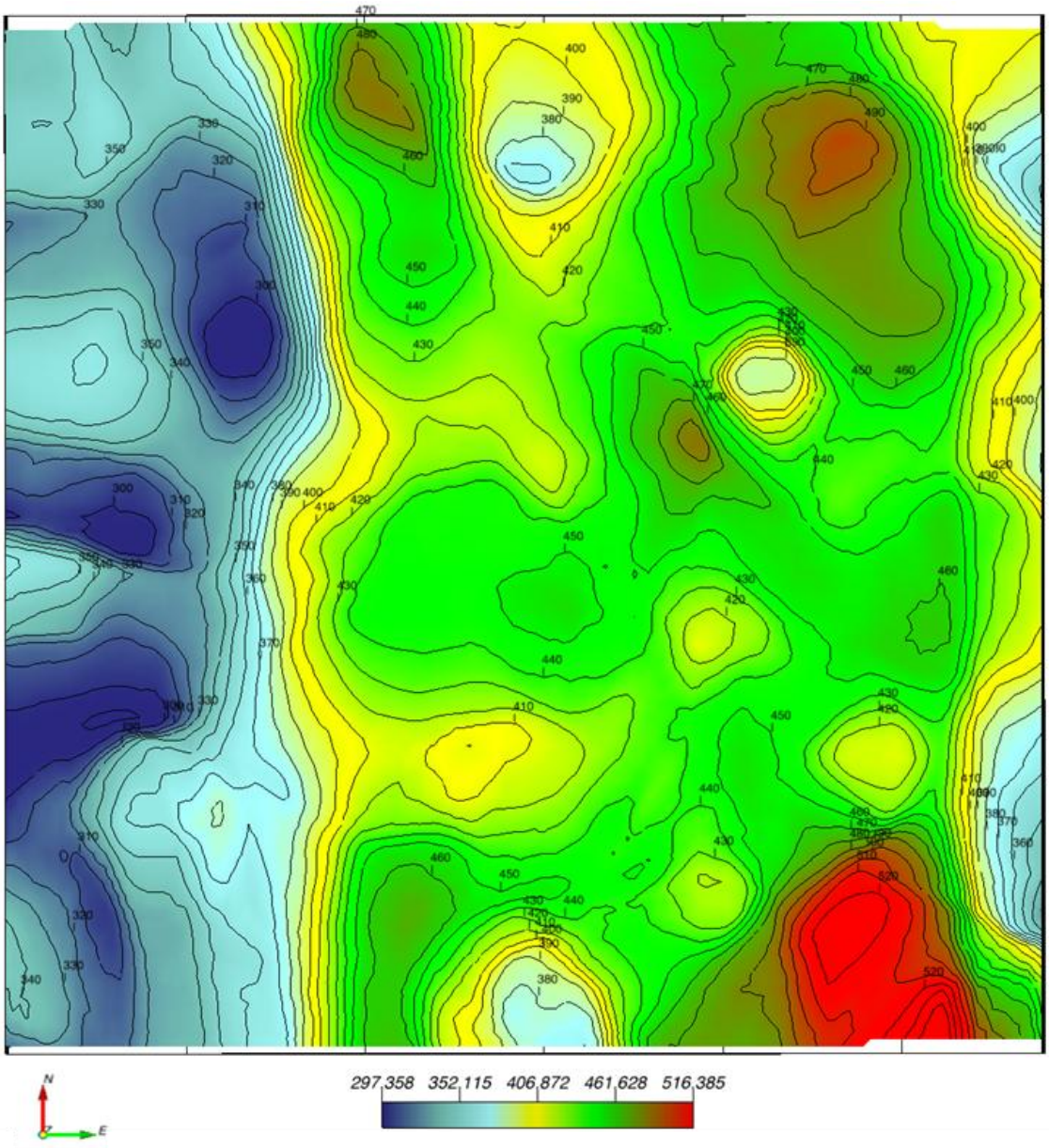

Figure 30. Isopach map showing the true stratigraphic thickness from the top of the Upper Fayetteville to the top of the Boone.

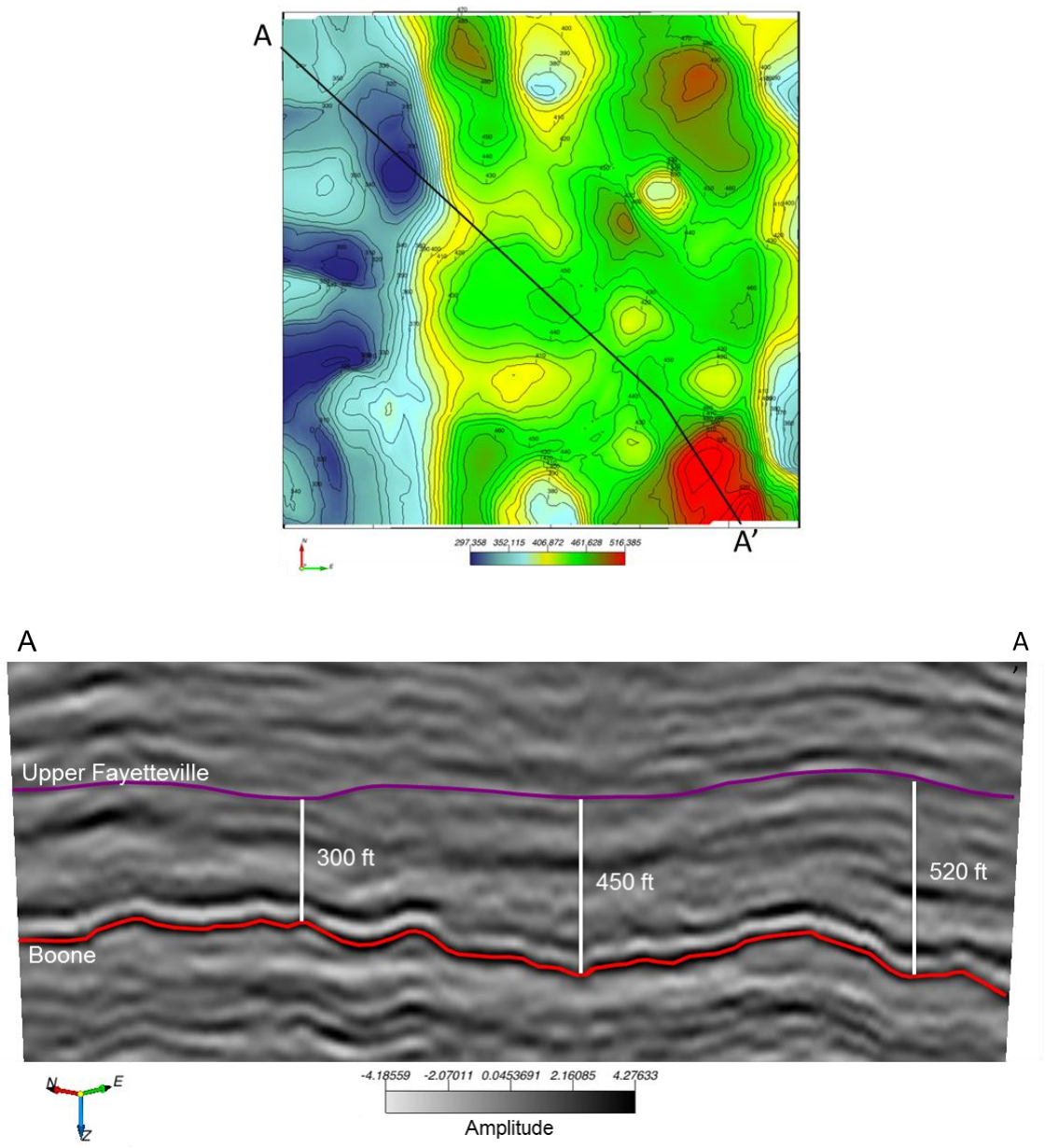

Figure 31. Cross-section of AA' from isopach map displaying the stratigraphic thickness from top of Upper Fayetteville to top of Boone.

B. Sinkhole Analysis

The total 3D seismic survey area is 9 mi^2 or 5,760 acres (Table 3). The average sinkhole area is 44.2 acres and the total sinkhole area is 618.9 acres, or 10.7% of the survey area. This number is conservative because possible sinkholes on the edges of the data are not included in the total. Figure 32 shows the sinkhole area distribution. The area is widely distributed and skewed to the left. Sinkhole 1 is the outlier and has the largest area of 5,076,643 ft^2 (471,635 m^2). Most are single sinkholes with the exception of sinkhole 1, 3, and 4 that appear to be multiple sinkholes that have coalesced.

Paleokarst Sinkhole Statistics			
Parameters	**Feet**	**Meters**	**Acres**
Average Sinkhole Area	1,925,741 ft^2	178,907 m^2	44.2
Total Sinkhole Area	26,960,379 ft^2	2,504,701 m^2	618.9
Average Depth	30	9.14	
Average Feret's Diameter	2,074	632	
Average Feret's Minimum Diameter	1,361	415	
Average Perimeter	6,120	1,865	
Average Circularity	0.635	0.635	
Desoto Survey Total Area	250,905,600 ft^2	23,309,893 m^2	5,760
% Total Area of Sinkholes	10.7	10.7	

Table 3. Statistics for the paleokarst sinkhole measurements.

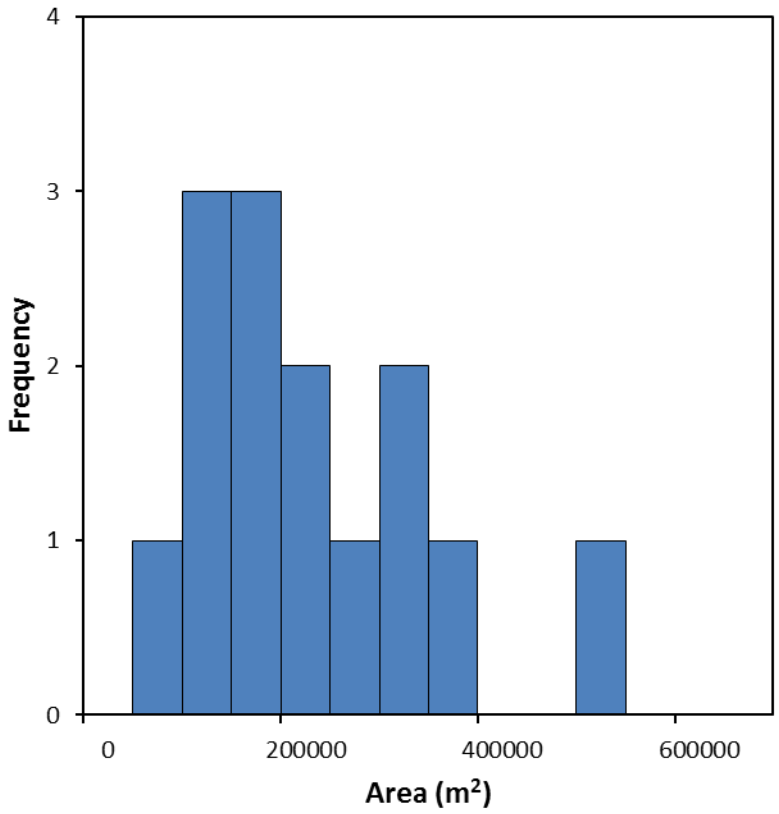

Figure 32. Distribution of sinkhole area.

The average size indicates observed sinkholes are very wide and shallow, with an average depth of 30 ft (9.14 m) deep. Because these sinkholes have an irregular shape and not a perfect circle, the length was measured by finding the Feret's diameter. The Feret's diameter is a group of diameters derived by finding the distance of two parallel lines in a defined orientation (Scientific Forum, 2016). The longest and shortest distance between any two points along the parallel planes are computed, known as Feret's diameter and Feret's minimum diameter. An example for this configuration is shown by Figure 33. The average Feret's diameter resulted in 2,074 ft (632 m) with an average perimeter of 6,120 ft (1,865m). A histogram of sinkhole Feret's diameters is shown in

Figure 34. The diameter ranges from 871 ft (265 m) to 3,671 ft (1,118 m). The histogram shows that the data is symmetrical as it revolves around the highest frequency range between 600-800 meters.

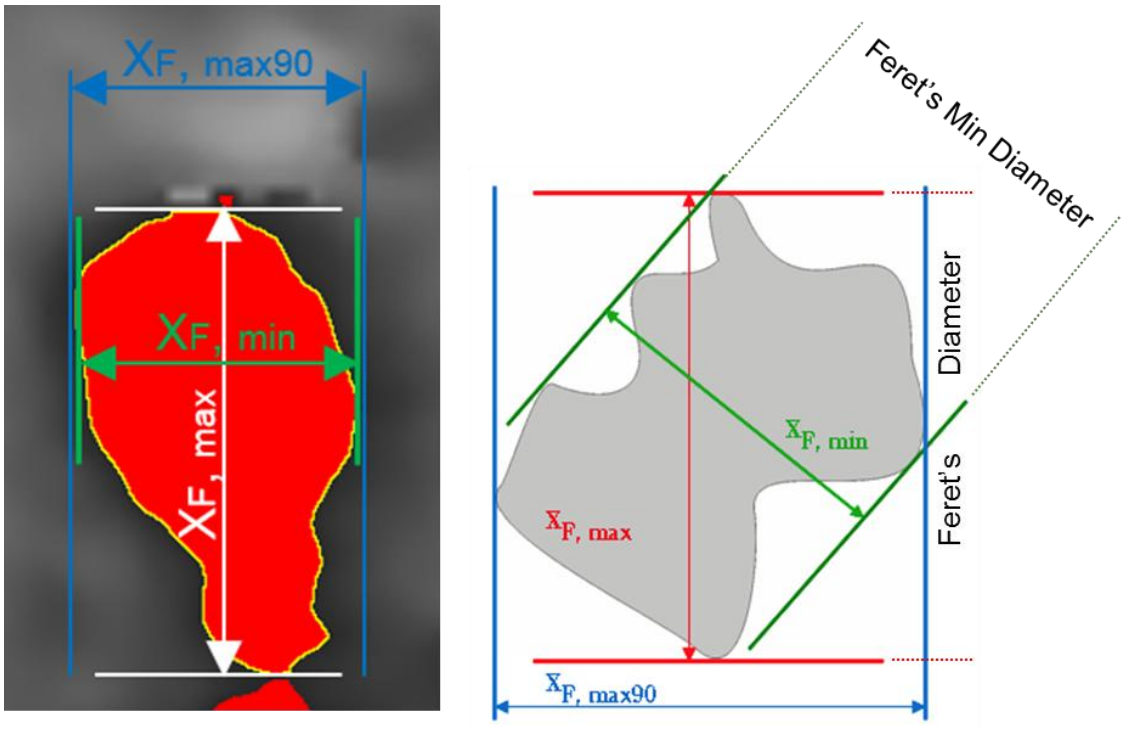

Figure 33. Ellipse of Sinkhole 1 in ImageJ, showing the configuration to estimate the Feret's Diameter. Modified from (Scientific Forum, 2016).

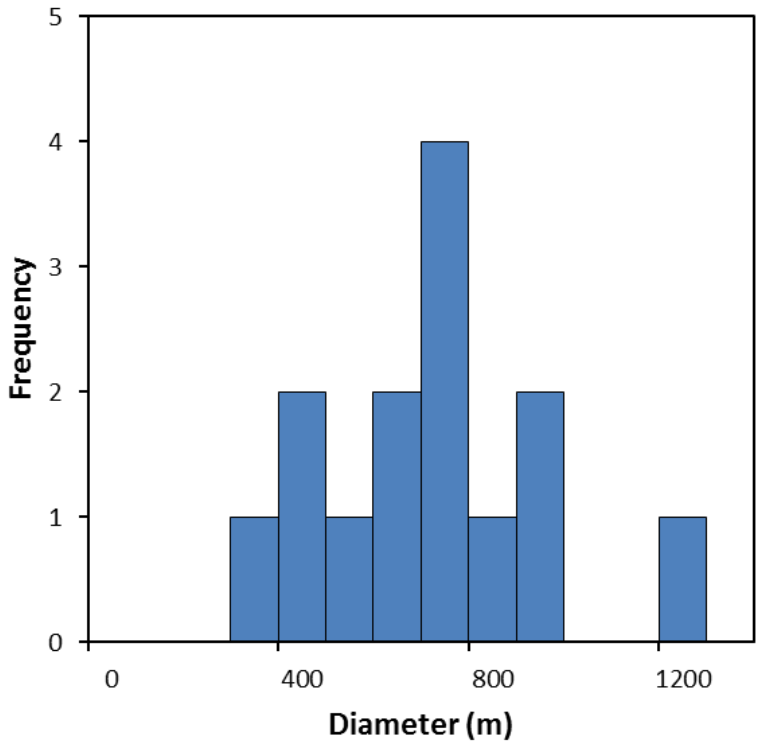

Figure 34. Distribution of sinkhole Feret's diameter

Quantifying the size is important to determine the type of the sinkhole. Figure 15 lists the six main types of sinkholes and their typical max size. Since the average Boone sinkhole in this study is 632 m across, they are only consistent with being solution sinkholes. The sinkhole mostly associated with the ones in the Boone Formation is a solution sinkhole formed from dissolutional lowering of a limestone and can be up to 1000 m across and up to 100 m deep (Waltham *et al*., 2005). Only one sinkhole was less than 300 m across (sinkhole 12), which could put it into the category of collapse or caprock sinkhole. However, it may just be a smaller solution sinkhole.

Sinkhole perimeter was found by calculating the entire length of the outside boundary. Figure 35 displays the histogram distribution for the perimeter values. With an

average perimeter of 6,120 ft (1,865 m), the distribution is bimodal with one grouping centered on 1,500 m and another at 2,750 m.

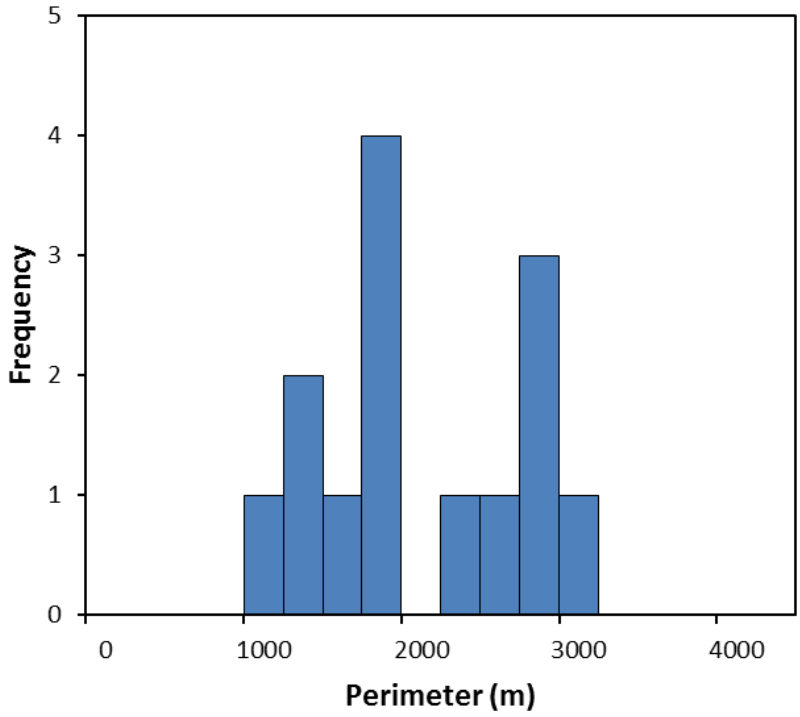

Figure 35. Distribution of sinkhole parameter.

Feret's diameter has a weak correlation with the sinkhole depth (Figure 36). The sinkholes become moderately deeper as they increase in size. In solution sinkholes, the depth and diameter are related. The diameter is enlarged as soil water infiltrates into the numerous points of the bedrock fissures (Figure 15b) and deepens the sinkhole across the entire floor with a saucer profile (Waltham *et al*., 2005). The deeper the depression, the greater amount of dissolutional points along the bedrock to potentially widen. With

continuous drainage towards the central sink of the doline, it deepens and develops a steeper, conical profile (Waltham *et al*., 2005).

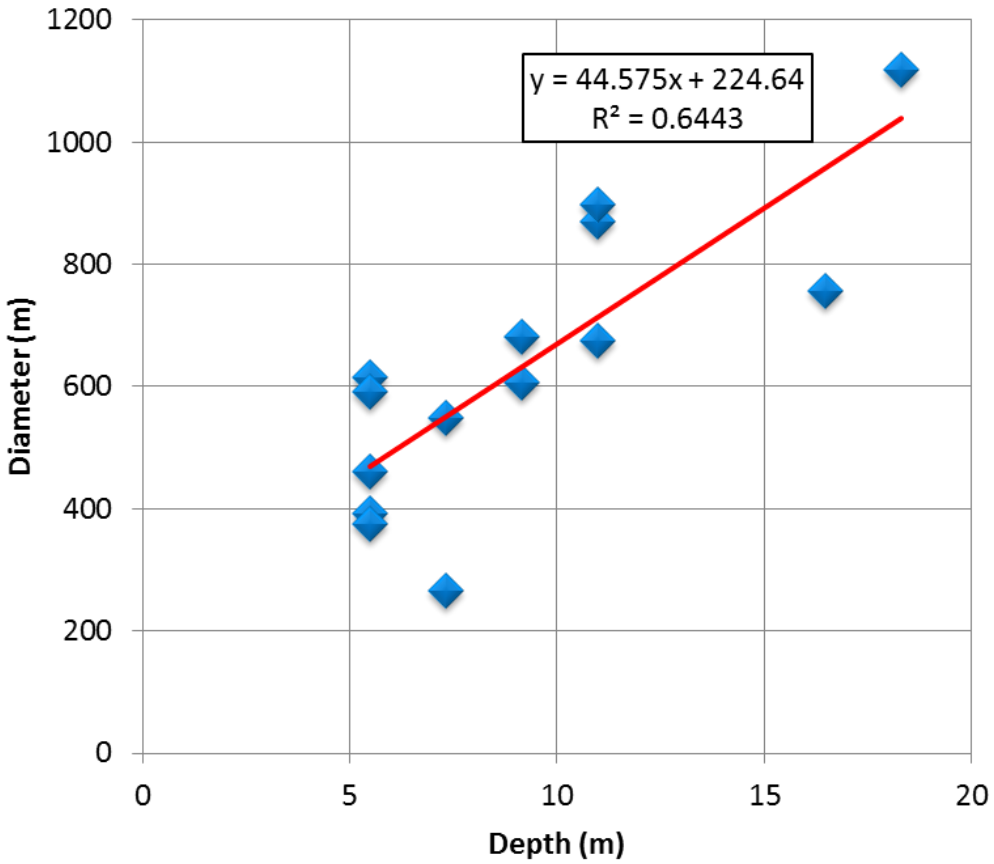

Figure 36. Boone sinkhole diameter-depth correlation.

Karst depressions typically have an approximately circular, bowl-like shape. To evaluate the circularity of the sinkholes, ImageJ defines a circularity index where 1.0 is a perfect circle and as the index approaches 0, the shape becomes increasingly elongated. A histogram of the distribution of the circularity index is seen in Figure 37. The index ranges from 0.307 to 0.849, has a mean value of 0.635, and a standard deviation of 0.147. The data is skewed to the right, with the majority of sinkholes having a circular index of 0.5 or greater. This indicates most Boone sinkholes are more circular than irregular. The highest circular index has a value of 0.849 for sinkhole 12. This is also the smallest sinkhole, which may indicate it being the youngest sinkhole out of the 14. Two of the lowest circularity index values were in sinkholes 3 and 4, exhibiting a value less than 0.5. Their shapes are irregular because they had coalesced with other sinkholes. According to Brinkmann *et al*., (2008), these are likely the oldest two sinkholes in the area because landscapes with individual circular depressions are younger than landscapes where sinkholes have coalesced.

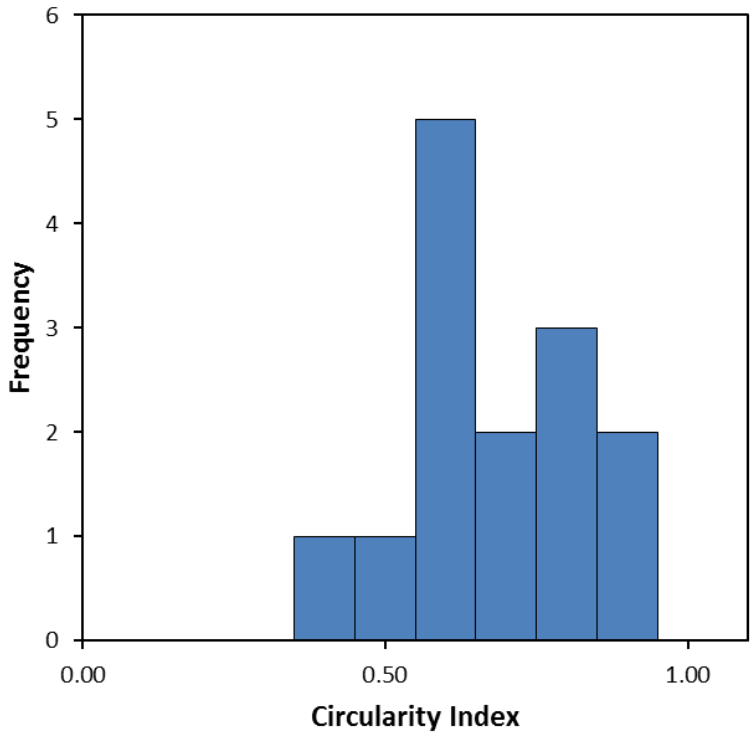

Figure 37. Distribution of the circularity index.

Based on the analysis, the sinkholes are most likely solution sinkholes. In the survey, the solution sinkholes and hills expand across the entire Boone surface and intertwine with each other. This kind of system in known as polygonal karst or cockpit karst (Waltham *et al*., 2005). Cockpit karst is common in tropical, humid environments and such landscapes have been recognized in Jamaica. The size of the hills are contingent on the maturity of the sinkholes. As dissolution increases and deepens the sinkholes, the "interfluve nodes are left as remnant hills" (Waltham *et al*., 2005). The Boone structure maps (Figures 22 and 23), indicate that sinkholes in the Boone Limestone terrain are consistent with polygonal karst morphology.

C. Fault Interpretation

Two faults have been mapped that propagate through the Boone Limestone, Moorefield Shale, Hindsville Limestone, and halfway through the Lower-Middle Fayetteville Shale shown by Figure 21. They strike east-west and are down to the south, offsetting the formations by about 60 ft. Faults in this area became active towards the end of Mississippian time due to Ouachita thrust loading as the rifted plates began to converge. In the eastern Arkoma Basin, faults are likely to extend all the way from the Upper Mississippian to the Proterozoic basement. Figure 38 shows the location of these faults on the Boone structure map. The image is a 3D perspective to help visualize the karst landscape. Assuming the depression in the southeast corner is a sinkhole, the largest sinkholes in the area are adjacent to faults. Faults are commonly associated with karst features, an example being the Ellenburger Group of the Fort Worth Basin, where faults control most of the large karst features (Qi *et al*., 2014). The fault-controlled karst in the Fort Worth Basin creates drilling hazards in the overlying Barnett Shale reservoir. Drilling interaction within these karst-related joint sets can produce large amounts of water because faults act as conduits for meteoric fluids (Qi *et al*., 2014), leading to increased dissolution along the joints, fractures, and into the bedrock.

It is not likely that the faults in the Desoto area enhanced dissolution because they were not active until the end of the Mississippian.

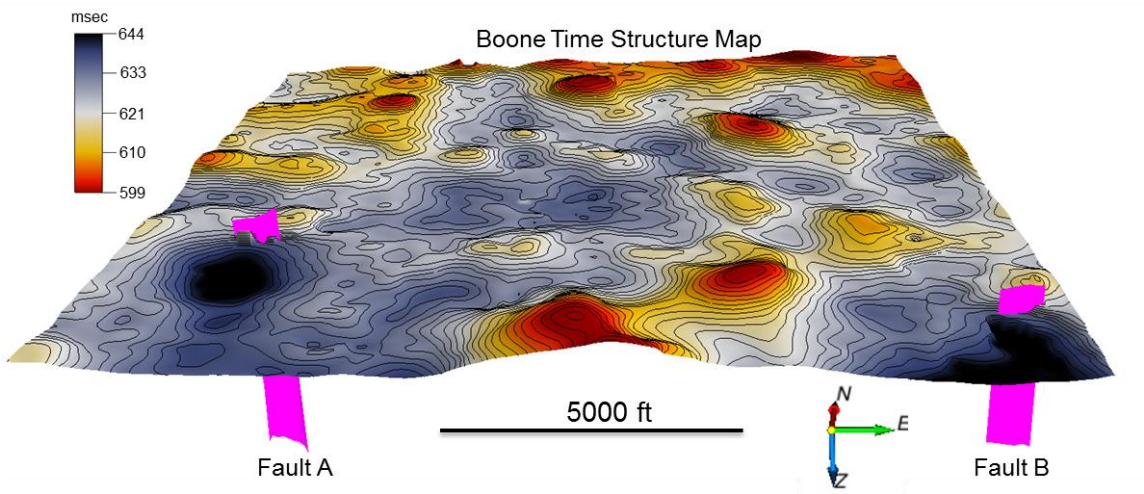

Figure 38. Time structure map of the Boone Formation displaying the two faults in the survey area.

D. Rock Characteristics

Rock properties can help identify areas of dissolution. A useful rock property related to lithology and porosity is acoustic impedance, defined as the product of velocity and density. Acoustic impedance in carbonates will be lower for rocks that have developed secondary porosity via dissolution.

The SWN acoustic impedance volume was extracted along top of the Boone, Moorefield, and Hindsville (Figure 39), and an outline for each sinkhole was overlaid onto the maps. Sinkholes in the Boone Formation typically show low acoustic impedance compared to their surroundings. The Boone outside sinkholes generally has a higher acoustic impedance because it has been physically and chemically less altered. This effect is particularly evident for sinkhole 1. Similar observations have been made in the karsted limestones of the Ellenburger formations (Fernandez and Marfurt, 2013). In the Moorefield Shale, we expect no relationship between acoustic impedance and sinkhole locations since all karst activity is at the Boone level. However, larger sinkholes that were infilled by the Moorefield Shale show a higher acoustic impedance compared to their surroundings. The difference is very subtle, but the change in acoustic impedance within the sinkholes may be a result of compaction. Results varied for the smaller sinkholes. In the Hindsville Limestone, the same results were evident. Stratigraphic termination near sinkholes 3 and 4 could have been from dissolution, indicated by low acoustic impedance.

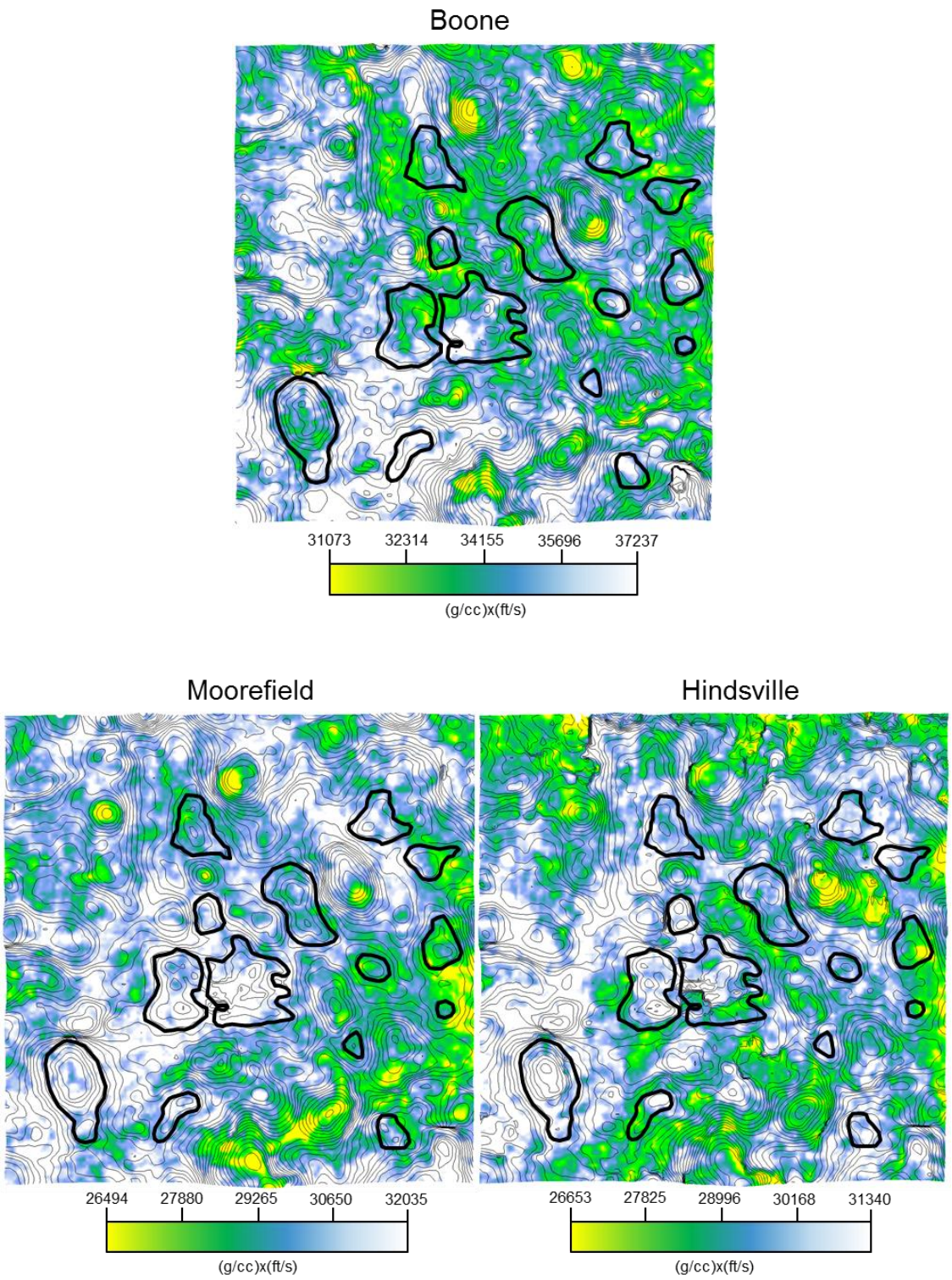

Figure 39. Acoustic impedance maps with outlined sinkholes.

E. Volumetric Curvature Characteristics

Many published seismic interpretations of sinkholes use volumetric curvature attributes to enhance structural features that are too small to detect in seismic amplitude data. Curvature is the reciprocal of the radius of a curve: K = 1/R. Roberts (2001) defines curvature as a "two-dimensional property of a curve that describes how bent a curve is at a particular point, or how much it deviates from a straight line." To visualize this concept, Figure 40 shows a 2D model of volumetric curvature.

The curvature attribute that was most useful in this study was most positive curvature (MPC). In Figure 41, the MPC is displayed for the Boone Formation. It has a 60% transparency overlay on top of the time structure map to gain a better visual of the surface. Positive MPC values represent the top of anticlines, ridges, or hills. Negative MPC values show the bottom of synclines, valleys, or sinkholes. Any flat or dipping surface will have a value of zero. Applying MPC shows that the landscape in the Boone Limestone is dominated by a system of sinkholes, hills, and ridges. An enlarged section was taken from the center of the surface in a non-transparent MPC view. Each white area represents a sinkhole on the Boone Limestone surface. The percentage of paleokarst sinkholes in the area appears to be much larger than the 10.7% previously calculated. For future studies, one could do an analysis covering the sinkholes shown in Figure 41 to get a more accurate percentage.

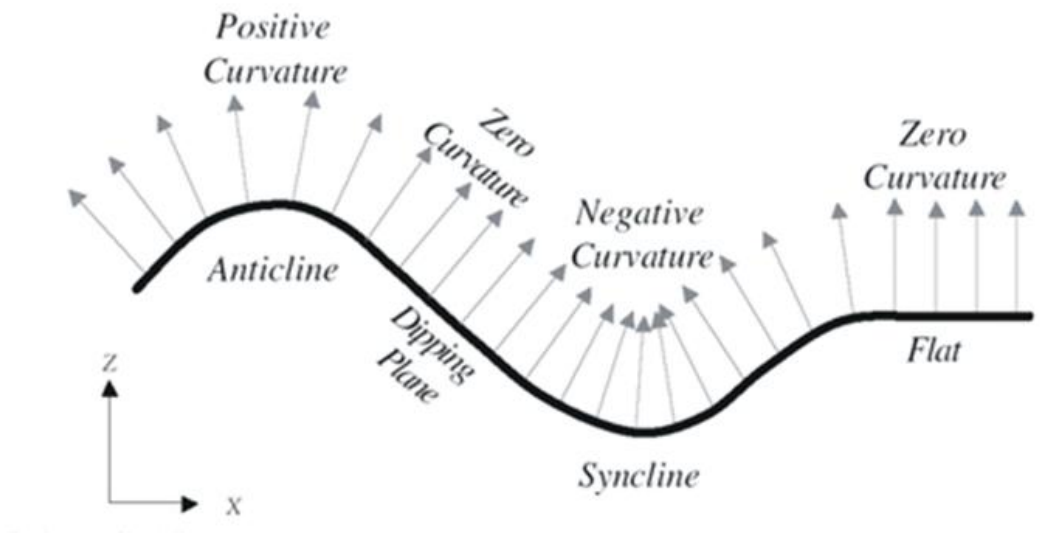

Figure 40. 2D model displaying the concepts of volumetric curvature (Roberts, 2001).

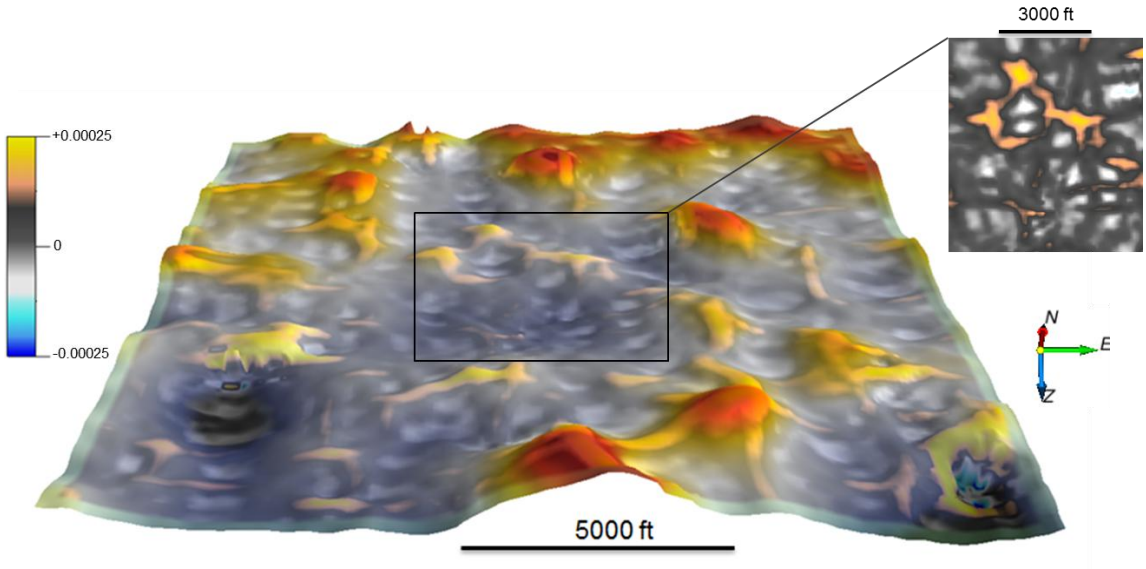

Figure 41. Most positive curvature map of the Boone Formation with a 60% transparency overlay on top of Boone time structure map.

F. Sinkhole Evaluation

Based on the seismic interpretation of the Mississippian units, it can be concluded that the sinkholes formed in the Boone Limestone. Following Boone deposition, sea level regressed across the southern midcontinent and exposed the carbonate surface to form sinkholes during this time of subaerial exposure. While sea level was relatively low, a thin low-stand wedge of Moorefield Shale (Meramecian-Early Chesterian) was deposited from the east in areas adjacent to the Mississippi Embayment. Because the shale was too thin to completely infill the sinkholes, the Moorefield depositional record exhibits the same topographic landscape as the Boone. A rise in sea level followed and initiated carbonate deposition of the Hindsville Limestone. Succeeding Batesville Sandstone deposition was confined to the shoreface environment as continuing transgression produced a thick layer of Lower-Middle Fayetteville Shale. This black shale exhibits east-to-west delivery and was thick enough to cover and fill the majority of the sinkholes. When sea level reached highstand conditions, deposition of the Upper Fayetteville filled in the remainder of the sinkholes and thickened the entire interval. There were no collapse features found in the Moorefield or Hindsville, which implies that dissolution occurred before these formations were deposited. These layers preserve the exact landscape that had formed on the Boone Formation.

Although precipitation during the Carboniferous was the highest at the beginning of the Pennsylvanian, it is very unlikely the sinkholes formed at the post-Kaskaskia unconformity. Meteoric waters would have had to penetrate through approximately 400 feet of Chesterian shales to reach the Boone limestone, which is implausible. Just as Palmer and Palmer (1989) specified, the earliest karst event during the Carboniferous

occurred after the Osagean epoch. This clarification requires an interpretation of how sinkholes could have formed during a hot and arid environment. In the early Mississippian, terrestrial vegetative cover in the southern mid-continent became extensive, and produced very high concentrations of CO_2 in both the atmosphere and the accumulating sedimentary record. Atmospheric carbon dioxide produces acidic rain, and even a small amount of precipitation falling on a carbonate terrain would quickly cause dissolution of the Boone bedrock, enhanced by biogenic CO_2 (Waltham *et al*., 2005). Sinkhole solution and collapse must have occurred during latest Chesterian and Meramecian time, which is represented by a regional unconformity at the top of the Boone across most of the Northern Arkansas Structural Platform. Upon subaerial exposure, solution and collapse became inactive during the deposition of the Moorefield and later stratigraphic intervals.

As it has been previously mentioned, sinkholes in the Boone limestone have been recognized in outcrops or on the surface in the Ozark region. It has been verified that sinkholes in the Boone limestone have also been preserved in the subsurface further south. This gives evidence that sinkholes could have developed further north in areas where the Boone had been deposited. Figure 3b shows a sinkhole in the Lower Ordovician that had been preserved and filled in by Pennsylvanian sediments. It is very likely that sinkhole development could have occurred in the Boone before the Mississippian formations were eroded away. In figure 42, a crossline seismic section is displayed that intersects the largest sinkhole in the survey area (sinkhole 1). The red arrow points out similar depression features underlying the Boone. Although there are not well logs deep enough to correlate the underlying strata, it is possible these structures are

sinkholes as well. In this case, it is possible that the sinkholes in the subsurface could reveal the depositional history of the missing Mississippian section in Rolla, Missouri. Another possibility is “time sag” resulting from Lower Fayetteville infill of the Boone sinkhole.

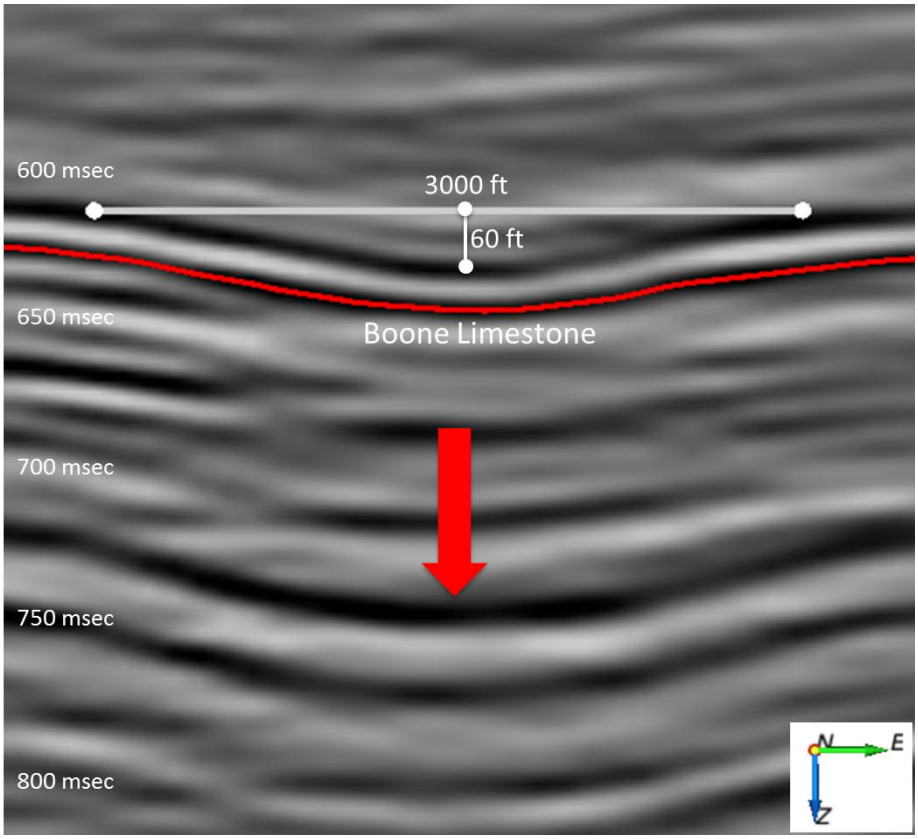

Figure 42. Seismic section showing similar depression features in lower formations. Crossline 1619.

CONCLUSIONS

The objective for this research was to further subsurface investigations in the eastern Arkoma Basin using 3D seismic. After analyzing the seismic data, numerous structural depressions were discovered in the Mississippian formations. Consequently, the main focus of this research was to analyze the features in the Mississippian to determine if the depressions were associated with paleokarst sinkholes. This was done by seismically mapping the tops of each surface in OpendTect. From time structure maps, it was quickly determined that the structures were related likely to sinkholes in the Boone Limestone based on their enclosed depressions. The study shifted into focusing on an analysis of the sinkholes and the depositional effects from the overlying layers.

A total of 14 sinkholes were recognized in the Boone depth structure map. By using ImageJ, it was possible to estimate the size and shape characteristics for each individual sinkhole. The results estimated that sinkholes occupied 10.7% of the entire 3D seismic survey area, probably an underestimation due to edge effects. When applying the MPC attribute, it appeared that the sinkhole population was over 50% across the carbonate terrain.

Future recommendations include a second analysis that could be applied to the MPC map of the Boone to get a more accurate percentage of sinkholes in the survey area. Despite the low estimation, it was determined that sinkholes in the area are solution sinkholes. The landscape of the Boone consisted of intersecting sinkholes and remnant hills. This polygonal organization portrays the characteristics of a cockpit karst landscape displayed in tropical humid environments.

Mapping all of the Mississippian formations was important in the research to understand when these sinkholes had formed and when they were finally filled. Because there was no sign of collapse in the Moorefield or Hindsville, formation of the sinkholes occurred after Boone deposition, when sea level regressed across the southern midcontinent and exposed the carbonate shelf. There was enough carbon dioxide in the atmosphere during the early Carboniferous for small amounts of precipitation and soil biogenic action to cause dissolution and chemically alter carbonates. These areas of higher dissolution were reflected by low acoustic impedance values in the Boone. Because the Moorefield and Hindsville were too thin to completely fill in the sinkholes, their depositional record exhibits the same topographic landscape as the Boone. Deposition of the Lower-Middle Fayetteville filled most of the sinkholes from the Early Mississippian. When sea level reached highstand conditions, deposition of the Upper Fayetteville filled in the remainder of the sinkholes and thickened the entire interval.

REFERENCES CITED

Blakey, R. C., 2008, "Paleogeography and Geologic Evolution of North America." *Nam.html*. Web. 20 Nov. 2015.

Boggs, S., 2012, Principles of sedimentology and Stratigraphy, Upper Saddle River, N.J., Pearson Prentice Hall, 662 p.

Borzenkova, I.I., and Turchinovich, I.Y., 2009, "History of Atmospheric Composition." Environmental Structure and Function: Climate System. Vol. II. Gruza, G., V., ed. 2009, p. 184-205.

Brinkman R, Parise M, and Dye, D., 2008, Sinkhole distribution in a rapidly developing urban environment: Hillsborough County, Tampa Bay area, Florida. Eng Geol 99 (3–4):169–184.

Chandler, Angela, 2013, Geology of the Big Flat and Buffalo City Quadrangles, Baxter, Marion, and Searcy Counties, Arkansas: Arkansas Geological Survey, map.

Coleman, Jr., J.L, 2000, Carboniferous Submarine Basin development of the Ouachita Mountains of Arkansas and Oklahoma, in A.H. Bouma and C.G. Stone. Eds., Fine-grained turbidite systems, AAPG Memoir 72/SEPM Special Publications. 68, p. 21-32.

EIA, "Shale News." Fayetteville Shale. N.d. Web. July 2016. Available at http://www.gulfoilandgas.com/webpro1/unconventional/oil-gas-shale.asp?id=14.

Esteban, M., and Klappa, C.F., 1983, Subaerial exposure environment. – IN: P.A., Bebout, D.G., Moore, C.H, (ed.): Carbonate depositional environments. – Mem. Am, Ass. Petrol. Geol., 33, p. 1-54.

"Fayetteville: The Shale Gale Reaches Arkansas." D.d. Web. Dec. 2015. Available at http://oilindependents.org/fayetteville-the-shale-gale-reaches-arkansas-3/

Fernandez, A., and Marfurt, K., (2013, May). *Detailed Seismic Characterization of a Heavily Karsted Zone*. Poster session presented at the AAPG Annual Convention and Exhibition, Pittsburgh, PA.

Ford, D. C., and Williams, P.F., 1989, Karst Geomorphology and Hydrology, London: Unwin Hyman, 576 p.

Horton, S., 2012, Disposal of Hydrofracking Waste Fluid by Injection into Subsurface Aquifers Triggers Earthquake Swarm in Central Arkansas with Potential for Damaging Earthquake: Seismological Research Letters, v. 83, no. 2, p. 250-260.

Houseknecht, D. W., 1986, Evolution from passive margin to foreland basin: the Atoka Formation of the Arkoma Basin, south-central U.S.A: Spec. Publs. int. Ass. Sediment., 8, 327-345.

Houseknecht, D.W., and Kacena, J.A., 1983, Tectonic and sedimentary evolution of the Arkoma foreland basin, in D.W. Houseknecht, ed., Tectonic-sedimentary evolution of the Arkoma Basin: SEPM Midcontinent Section Guidebook, v. 1, p. 3-33.

Houseknecht, D.W., Rouse, W.A., Paxton, S.T., Mars, J.C., and Fulk, B., 2014, Upper Devonian-Mississippian stratigraphic framework of the Arkoma Basin and distribution of potential source-rock facies in the Woodford-Chattanooga and Fayetteville-Caney shale-gas systems. AAPG Bulletin, v. 98, no. 9, p. 1739-1759.

James, N. P. and Choquette, P.W., 1984, Diagenesis 9. Limestones-the meteoric diagenetic environment. Geoscience Canada, v 11, p161-194.

Kumbalek, M. 2015. Analysis of paleokarst sinkholes in the Arkoma Basin using 3-D seismic (Order No. 1586791). Available from ProQuest Dissertations & Theses Global.

Liner, Christopher L., 2004, Elements of 3D Seismology. 2nd ed. Tulsa, OK: PennWell, 2004. Print.

Manger, W.L., 2015, Introduction to the Upper Mississippian (Chesterian) Geology of the Southern Ozarks, Northern Arkansas. *Southwestern Energy Company Summer Intern Program Desoto Geology Fieldtrip Guidebook.* Print

Maslyn, R. M, 1977, Recognition of Fossil Karst Features in the Ancient Record: A Discussion of Several Common Fossil Karst Forms, IN Veal, H.K., ed., Southern and Central Rockies Exploration Frontiers: Rocky Mtn. Assoc. Geologists Guidebook, p. 311-319

Moore, C.H. and Wade, W.J. 2013, Carbonate Reservoirs: Porosity and diagenesis in a sequence stratigraphy, second edition, Elsevier, 170 p.

Ozark Plateaus: Mississippian. N.p., n.d. Web. 21 Jan. 2016. <http://www.geology.ar.gov/geology/ozark_mississippian.htm>

Palmer, M.V., and Palmer, A.N., 1989, Paleokarst of the United States. *Paleokarst: A systematic and Regional Review*. P. Bosak, D.C. Ford, J. Glazek, I. Horacek, (ed.) New York, Elsevier, 1989. p. 337-361.

Perry, W. J. , 1994, *Arkoma Basin Province (062)*, IN D. L. Gautier, G. L. Dolton, K. I. Takahashi and K. L. Varnes, eds., 1995 National assessment of United States oil and gas resources — Results, methodology, and supporting data: U.S. Geological

Survey Digital Data Series 30, CD-ROM.

Qi, J., Zhang, B., Zhou, HL., and Marfurt, K., 2014, Attribute expression of fault-controlled karst-Fort Worth Basin, Texas: A tutorial. Interpretation: A Journal of Subsurface Characterization. v. 2, iss. 3, p. SF91-SF110.

Rascoe, B., Jr. and Adler, F.J., 1983, Permo-Carboniferous hydrocarbon accumulations, mid-continent U.S.A.: American Association of Petroleum Geologists Bulletin, v. 67, p. 979-1001.

Ratchford, M. E., and L. C. Bridges 2006. Geochemistry and thermal maturity of the Upper Mississippian Fayetteville Shale Formation, eastern Arkoma Basin and Mississippi Embayment regions, Arkansas: Transactions - Gulf Coast Association of Geological Societies, v. 56, p. 717-721.

Roberts, A., 2001, Curvature attributes and their application to 3-D interpreted horizons. First Break, Wiley, v. 19 iss. 2, p. 85–100.

Rogers, R. (2012). Structural Evolution of the Eastern Arkoma Basin: Integrating a 3D Pre-stack Time Migration into the Preexisting Structural Framework. Master's Thesis, University of Houston. 60 p.

Scholle, P. A. and Ulmer-Scholle, D. S. 2003. A Color Guide to the Petrography of Carbonate Rocks: Grains, Textures, Porosity, Diagenesis, AAPG Memoir 77, AAPG.

Scientific Forum Particle Characterisation. *Sympatec's Scientific Forum.* N.p., n.d. Web. July 2016. Available at http://www.sympatec.com/EN/Science/Characterisation/05_ParticleShape.html

Shelby, P.R., 1986, Depositional history of the St. Joe and Boone Formations in northern Arkansas: Arkansas Academy of Science thesis, University of Arkansas, 92 p.

Suneson, N.H., 2012, Arkoma Basin Petroleum-Past, Present, and Future. Oklahoma City Geological Society. Oil and Gas Journal, v. 63, no. 1, p 38-70.

Sutherland, P., K., 1988, Late Mississippian and Pennsylvanian depositional history in the Arkoma Basin area, Oklahoma and Arkansas: Geological Society of American Bulletin, v. 100, no. 11, p. 1797-1802.

Taylor, Larry. "Fayetteville Shale - Encyclopedia of Arkansas." Web. 18 July 2016.

VanArsdale, R. B., and E. S. Schweig III, 1990, Subsurface Structure of the Eastern Arkoma Basin: American Association of Petroleum Geologist Bulletin, 74, 1030-1037.

Viele, G. W. 1973, Structure and tectonics of the Ouachita Mountains, IN K. DeJong and R. Schollen, (eds.), *Gravity and tectonics*: New York, Wiley, p. 361-377.

Waltham Tony, F. G. Bell, and M. G. Culshaw, 2005, Sinkholes and Subsidence: Karst and Cavernous Rocks in Engineering and Construction. Berlin: Springer. Print.

Wright, V.P., and Smart, P.L. 1994, Paleokarst (dissolution diagenesis): its occurrences and hydrocarbon exploration significance. IN Ed. K.H. Wolf and G.V. Chilingarian. *Diagenesis, IV.* New York, p. 477-510.

APPENDIX

Shape Characteristics defined by ImageJ

Area: Area of selection in square pixels or in calibrated square units

Min & max gray level: Minimum and maximum gray values within the selection.

Centroid: The center point of the selection. This is the average of the x and y coordinates of all of the pixels in the image or selection. Uses the X and Y headings.

Perimeter: The length of the outside boundary of the selection.

Fit ellipse: Fits an ellipse to the selection. Uses the headings Major, Minor and Angle. Major and Minor are the primary and secondary axis of the best fitting ellipse. Angle is the angle between the primary axis and a line parallel to the X-axis of the image. The coordinates of the center of the ellipse are displayed as X and Y if Centroid is checked.

Circularity: $4\pi \times [\text{Area} / \text{Perimeter}^2]$ with a value of 1.0 indicating a perfect circle. As the value approaches 0.0, it indicates an increasingly elongated shape. Values may not be valid for very small particles.

Feret's diameter: The longest distance between any two points along the selection boundary, also known as maximum caliper. Uses the heading Feret. The angle (0--180 degrees) of the Feret's diameter is displayed as Feret Angle, as well as the minimum caliper diameter (Min Feret). The starting coordinates of the Feret diameter (Feret X and Feret Y) are also displayed

Aspect ratio: The aspect ratio of the particle's fitted ellipse: Major axis / Minor axis.

Roundness: $4 \times [\text{Area} / \pi \times (\text{major axis})^2]$ or the inverse of Aspect Ratio.

Solidity: [area / convex area]